A Durable, Intermediate Temperature, Direct Reading Heat Flux Transducer for Measurements in Continuous Wind Tunnels

C. T. Kidd
Calspan Field Services, Inc.

November 1981

Final Report for Period October 1, 1980 — June 30, 1981

ARNOLD ENGINEERING DEVELOPMENT CENTER
ARNOLD AIR FORCE STATION, TENNESSEE
AIR FORCE SYSTEMS COMMAND
UNITED STATES AIR FORCE

This report has been reviewed by the Office of Public Affairs (PA) and is releasable to the National Technical Information Service (NTIS). At NTIS, it will be available to the general public, including foreign nations.

APPROVAL STATEMENT

This report has been reviewed and approved.

MARSHALL K. KINGERY
Directorate of Technology
Deputy for Operations

Approved for publication:

FOR THE COMMANDER

MARION L. LASTER
Director of Technology
Deputy for Operations

REPORT DOCUMENTATION PAGE		READ INSTRUCTIONS BEFORE COMPLETING FORM
1 REPORT NUMBER AEDC-TR-81-19	2 GOVT ACCESSION NO	3 RECIPIENT'S CATALOG NUMBER
4 TITLE *(and Subtitle)* A DURABLE, INTERMEDIATE TEMPERATURE, DIRECT READING HEAT FLUX TRANSDUCER FOR MEASUREMENTS IN CONTINUOUS WIND TUNNELS		5 TYPE OF REPORT & PERIOD COVERED Final Report - Oct. 1, 1978 – June 30, 1981
		6 PERFORMING ORG REPORT NUMBER
7 AUTHOR(*s*) C. T. Kidd, Calspan Field Services, Inc.		8 CONTRACT OR GRANT NUMBER(*s*)
9 PERFORMING ORGANIZATION NAME AND ADDRESS Arnold Engineering Development Center/DOT Air Force Systems Command Arnold Air Force Station, TN 37389		10 PROGRAM ELEMENT, PROJECT, TASK AREA & WORK UNIT NUMBERS Program Element 65807F
11 CONTROLLING OFFICE NAME AND ADDRESS Arnold Engineering Development Center/DOS Air Force Systems Command Arnold Air Force Station, TN 37389		12 REPORT DATE November 1981
		13 NUMBER OF PAGES 62
14 MONITORING AGENCY NAME & ADDRESS(*If different from Controlling Office*)		15 SECURITY CLASS. *(of this report)* UNCLASSIFIED
		15a DECLASSIFICATION· DOWNGRADING SCHEDULE N/A

16. DISTRIBUTION STATEMENT *(of this Report)*

Approved for public release; distribution unlimited.

17 DISTRIBUTION STATEMENT *(of the abstract entered in Block 20, If different from Report)*

18 SUPPLEMENTARY NOTES

Available in Defense Technical Information Center (DTIC).

19. KEY WORDS *(Continue on reverse side if necessary and identify by block number)*

heat transfer	gages
temperature coefficients	aerodynamic heating
transducers	wind tunnels
heat flux	

20 ABSTRACT *(Continue on reverse side if necessary and identify by block number)*

    The design and development of a high durability, intermediate service temperature ($\leq 600^\circ F$), direct reading transducer for the measurement of aerodynamic heating in the continuous wind tunnels of the von Kármán Gas Dynamics Facility (VKF) of the Arnold Engineering Development Center (AEDC) is described. This transducer operates on the axial temperature gradient or Schmidt-Boelter measurement concept. Considerable emphasis is placed

20. ABSTRACT (Continued)

upon the practical use of a finite-element, two-dimensional heat conduction code for analysis of gage behavior rather than the indiscriminate use of invalid exact mathematical solutions. Laboratory evaluation and calibration of prototype transducers at ambient temperature levels varying from 70 to 500°F are discussed. Results of wind tunnel aerodynamic heating measurements using limited numbers of prototype Schmidt-Boelter gages are presented. Recommendations for future work efforts with regard to further development and testing of this measurement concept are discussed.

PREFACE

The work reported herein was performed by the Arnold Engineering Development Center (AEDC), Air Force Systems Command (AFSC), under Program Element 65807F. The Air Force project manager was M. K. Kingery. The results were obtained by Calspan Field Services, Inc. operating contractor for the Aerospace Flight Dynamics testing effort at the AEDC, AFSC, Arnold Air Force Station, Tennessee under AEDC Project No. D228VW (Calspan Project No. V32L-B21). The manuscript was submitted for publication on September 11, 1981.

The author wishes to acknowledge the contributions of W. T. Scott in the design and fabrication of the prototype transducers.

CONTENTS

ILLUSTRATIONS

TABLES

APPENDIX

1.0 INTRODUCTION

A wide range of aerodynamic heating measurement requirements exists at the von Kármán Gas Dynamics Facility (VKF) of the Arnold Engineering Development Center (AEDC), varying from atmospheric reentry conditions to the low supersonic Mach number regime of today's tactical aircraft (Ref. 1). Various sensors and techniques have been used over the past several years for the measurement of aerodynamic heating at the VKF (Refs. 2, 3, and 4). All of these sensors and techniques have one or more attractive operating characteristics, but no one sensor or technique is appropriate for all measurement applications. Efforts are continually directed toward upgrading the quality of aerodynamic heating measurements in the continuous wind tunnels of the VKF. Conventional and thermopile Gardon gages, coaxial surface thermocouples, and the thin skin technique have all been successfully employed in continuous wind tunnel measurement applications during the last twelve years. The thermopile Gardon gage (Ref. 2) has gradually evolved as the transducer generally used in discrete gage measurement applications at the VKF. Although the thermopile Gardon gage possesses several desirable operating features (good sensitivity, self-generating output directly proportional to incident heat flux, good accuracy, etc.) and has provided generally reliable test results, the gage has several deficiencies in this measurement application. These deficiencies include only fair durability, limited high service temperature (300°F maximum), somewhat temperature-dependent scale factor, and no contourability.

Technology efforts have been directed toward the design and development of a transducer which retains the desirable operating features of the thermopile Gardon gage and provides significant improvements in each of the deficient areas listed above. Substantial progress in the development of such a transducer has been achieved. This transducer operates on the Schmidt-Boelter or axial temperature gradient principle (Refs. 5, 6, and 7). Although there has been little previous experience and very sparse reporting with regard to this technique in aerodynamic heat transfer measurement applications, this measurement concept is not new. Most of the reporting of the Schmidt-Boelter gage has been in strictly steady-state applications with relatively large ($\geq$ 0.5-in.-diam by $\geq$ 0.25-in.-wafer thickness) sensors. A moderate degree of confusion exists within the technical community because of inconsistency among users, experimenters, and manufacturers with regard to terminology used when referring to this measurement concept. This report will be consistent with reference to the measurement concept described here as the Schmidt-Boelter gage.

As a result of technology efforts directed toward general improvements in heat transfer measurements in continuous wind tunnels, significant advances in heat flux gage development have been made, and a better general understanding of aerodynamic heat transfer

measurements has been achieved. Much of the success of the development of the Schmidt-Boelter gage concept into a practical transducer can be attributed to the use of a transient, finite-element, two-dimensional heat conduction code (Ref. 8) in gage analysis. This computer code permits the simultaneous consideration of up to 100 materials with different geometric configurations and thermal properties. Good agreement between analytical predictions of timewise temperature distributions within the gage obtained with the computer code and actual prototype gage behavior was achieved and is graphically illustrated in this report. These results are contrasted with inaccurate data obtained with exact equations whose mathematical models are not truly representative of the real gage. Careful selection of gage materials to achieve proper and predictable behavior is emphasized.

Prototype Schmidt-Boelter gages designed and fabricated to date have exhibited excellent durability in wind tunnel tests, can withstand continuous (8 hr) service temperature environments in the laboratory up to 600°F with no apparent detrimental effects, have a calibration scale factor which is essentially independent of temperature within the operating range, and are semicontourable. These gages have a heat flux sensitivity equal to or greater than thermopile Gardon gages of the same basic physical configuration and feature output signals directly proportional to the heat flux incident on the sensing surface of the transducer.

Measurement of aerodynamic heating in continuous wind tunnels involves all three of the well-known modes of heat transfer. In the case of the Schmidt-Boelter gage and most other techniques/sensors, aerodynamic (convection) heating is measured with a device which operates on the principle of heat conduction and is generally calibrated with a radiant heat source (quartz tube lamp bank). Subtle error-inducing mechanisms may be unwittingly incorporated into measurement or calibration systems. Thermophysical phenomena which contribute to measurement inaccuracies present in both operational and calibration environments must be identified and noted. A good understanding of the overall problem is essential to obtaining high quality wind tunnel data. Analysis of early wind tunnel data from Schmidt-Boelter gages prompted a gage modification with emphasis on minimizing possible surface temperature perturbations or discontinuities along the surface of the wind tunnel model.

The purpose of this report is to document the development of the Schmidt-Boelter gage concept as a practical heat transfer measurement device primarily for aerodynamic wind tunnel applications. Included are gage fabrication details, mathematical analyses, laboratory evaluation and calibration, and wind tunnel test results. Recommendations for further work to optimize gage performance and possible applications other than wind tunnel testing are discussed.

2.0 DESIGN

2.1 PRINCIPLE OF OPERATION

The principle of operation of the Schmidt-Boelter gage involves measuring the temperature difference, ΔT, between two parallel planes on the top and bottom of a slab or wafer which is backed by a heat sink, as illustrated in Fig. 1. This temperature difference is generally measured with a differential thermocouple. The hot junction temperature, T_H, is on the top surface of the slab and the cold junction temperature, T_C, is on the bottom surface. The material and thickness, ℓ, of the slab can vary widely; the heat sink is usually a material with a high thermal conductivity such as aluminum, copper, etc. Excellent sensitivity is achieved in the practical implementation of this measurement concept by employing a series thermocouple (thermopile) technique to detect the temperature difference, ΔT, between the two parallel planes, as shown in Fig. 2. For the design shown in Fig. 2, the thermopile is constructed by winding N turns of small diameter constantan thermocouple grade wire around the wafer. One-half of the coil assembly (top and bottom) is electroplated with copper, creating a multi-element copper-constantan differential thermocouple. This gage features a self-generating output signal, ΔE_o, which is directly proportional to the heat flux, $\dot{q}$, incident upon the sensing surface of the transducer. The steady-state output signal of the transducer is given by:

$$\Delta E_o = \dot{q} \cdot N \cdot \ell \cdot \delta / K \tag{1}$$

where δ and K are the thermoelectric sensitivity of the copper-constantan thermocouple and the thermal conductivity of the slab, respectively. Derivation of Eq. (1) is described in Sec. 3.1 and Appendix A.

A thermocouple is provided inside an actual gage to measure the bottom surface temperature, T_C, of the slab. This feature enables the Schmidt-Boelter gage to be used for aerodynamic heat transfer measurement applications. Construction details of the transducer developed for measurements in the continuous wind tunnels of the VKF are given in Sec. 2.3.

2.1.1 Data Reduction

Reduction of instantaneous heat flux data from the Schmidt-Boelter gage involves only multiplying the gage calibration scale factor by the timewise transducer output signal. This gives the user the heat flux incident on the surface of the transducer at any time point. It will be shown in Sec. 4.2.3.2 that the gage calibration scale factor is essentially independent of

transducer temperature, T_w, through the operating range of 70- 600°F. Often the parameter of interest to the experimental aerodynamicist is the heat transfer coefficient or Stanton number. Reduction of data to obtain these parameters involves a gage temperature measurement, as well as heat flux.

T_H – Top Surface Temperature

T_C – Bottom Surface Temperature
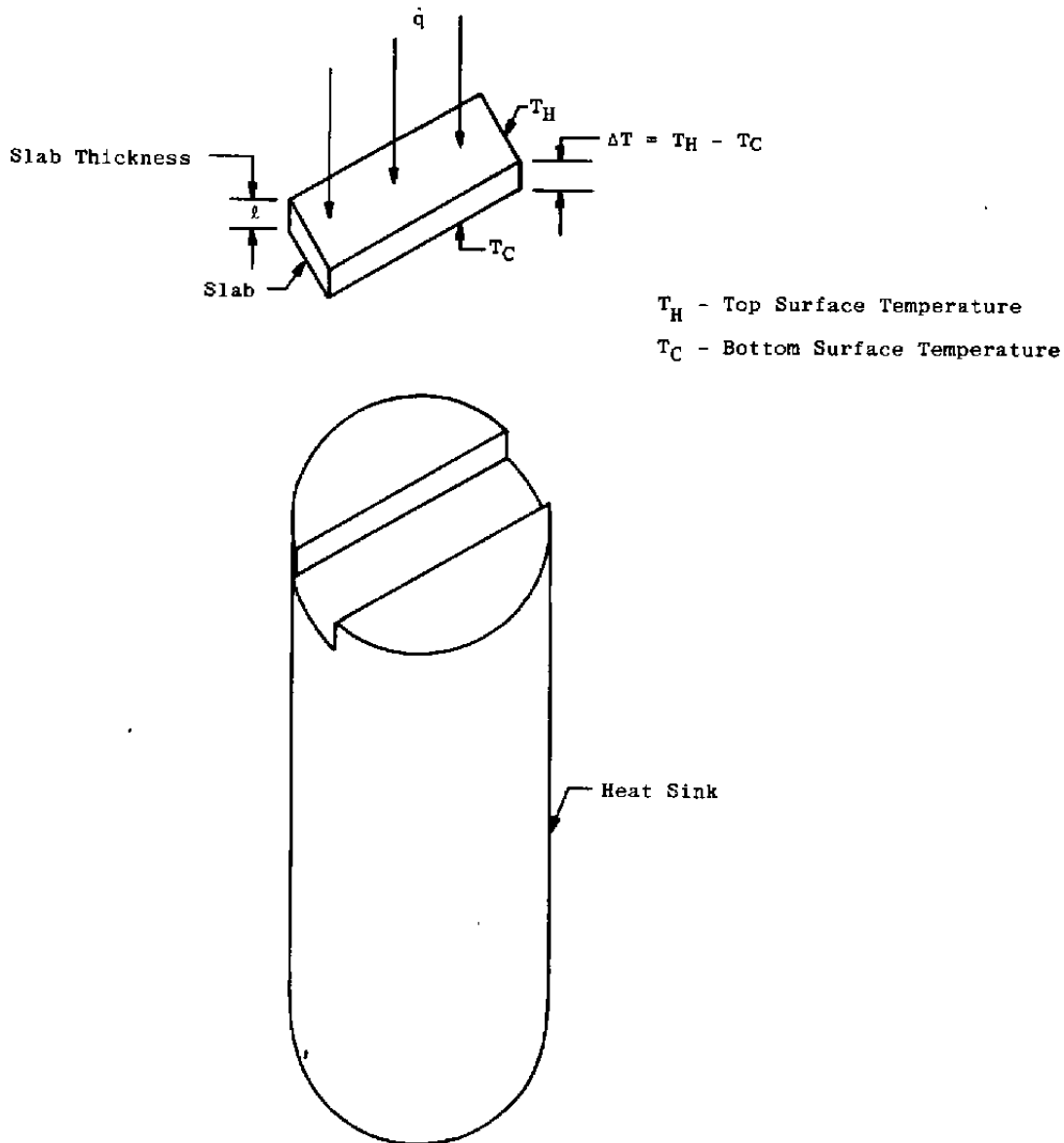
Figure 1. Schmidt-Boelter gage concept.
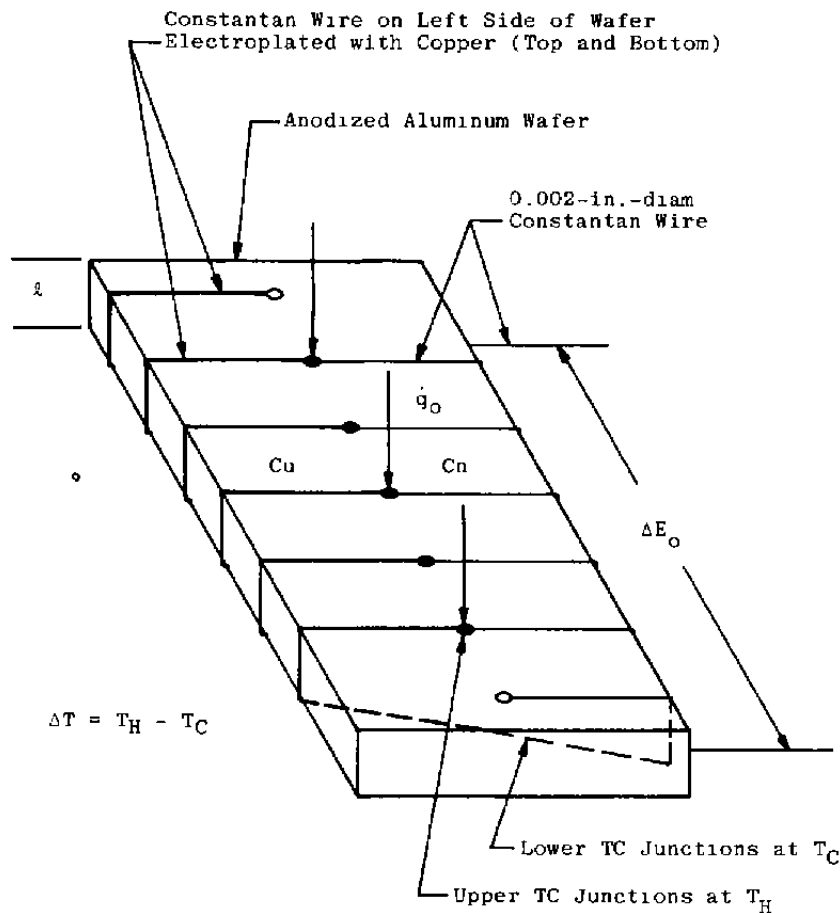
Figure 2. Differential temperature measurement concept of Schmidt-Boelter gage.

2.1.2 Aerodynamic Heating Measurement Applications

Although quite versatile in its potential overall application capabilities, the Schmidt-Boelter gage described in this report was designed primarily for the measurement of aerodynamic heating in continuous wind tunnels. The gage measures the heat flux incident on the sensing surface at any time point. A thermocouple from which the gage surface temperature history can be calculated (see Sec. 4.1.1) is contained within the gage. In general aerodynamic heating applications, the parameter of principal interest is the heat transfer coefficient, h, which is defined as:

$$h \equiv \dot{q}/(T_T - T_w) \tag{2}$$

Since both $\dot{q}$ and T_w are obtained from gage measurements, only the recovery temperature, T_r, need be determined to evaluate the heat transfer coefficient. The determination of the correct value of T_r is often a formidable task for the experimental aerodynamicist. It is an accepted practice (Ref. 4) in hypersonic flow to use a measured parameter, namely the stilling chamber temperature, T_T, in lieu of T_r; i.e.,

$$h \equiv \dot{q}/(T_T - T_w) \tag{3}$$

Relationships between T_r and T_T for both laminar and turbulent boundary layers are available in several aerothermodynamic references and texts (Ref. 9). The calculated value of heat transfer coefficient may be corrected by application of these relationships. This practice results in insignificant inaccuracies in the calculation of heat-transfer coefficient as long as T_w is small compared with T_T. However, for test situations where $T_T - T_w \leq 200°F$, the determination of h by the method described here is considered invalid. In these cases, heat-transfer coefficients can be accurately determined by a graphical method outlined in Ref. 4.

2.2 DESIGN CRITERIA

There are several performance factors which must be considered in the design of any heat flux transducer, including a Schmidt-Boelter gage whose principle of operation was described in the preceding section. These performance factors include method of data reduction, heat flux sensitivity, time response, front surface temperature rise, maximum continuous service temperature, change of calibration factor with temperature, physical size, contourability, and durability.

An ideal transducer for aerodynamic heat transfer measurement applications in continuous wind tunnels would have an output signal directly proportional to the heat flux incident on the sensing surface, a heat flux sensitivity ≥ 20 mv/Btu/ft²-sec, and a time response on the order of 0.10 sec. In addition, the ideal transducer would have a sensing surface temperature exactly the same as the adjacent model or test article surface, a maximum continuous service temperature of at least 1,500°F, and a calibration scale factor completely independent of ambient gage temperature. Physical characteristics of the transducer should include small size (≤ 0.125-in.-diam by ≤ 0.35 in.), ability to be contoured exactly to match a model surface, and ability to withstand any normal test environment with no structural damage. It may be possible to achieve one or more of these ideal performance factors with practical application of the Schmidt-Boelter concept; however, even an inexperienced gage designer would recognize that it would be virtually impossible to attain

all of these performance factors in one gage. Therefore, design tradeoffs have to be made. The procedure followed involved first setting minimum requirements for all performance factors and then adjusting certain design parameters to achieve optimum performance in the more critical areas. This procedure is outlined below:

Method of Data Reduction — The new transducer should have an output signal which is directly proportional to the heat flux incident upon the sensing surface.

Heat Flux Sensitivity — The 10-mil, 1/4-in.-diam thermopile Gardon gage (Ref. 2) has a sensitivity of approximately 2.0 mv/Btu/ft^2 -sec. The new transducer should have a sensitivity of at least that value.

Time Response — Previous continuous wind tunnel tests have shown that a time response of 1.0 sec to 95 percent of full scale is a minimum requirement.

Front Surface Temperature Rise — An important consideration in heat gage design is that the surface temperature of the gage be as close to the surface temperature of the adjacent model or test article as possible. This criterion should minimize temperature discontinuities along the surface as the tunnel flow progresses from the model surface to the gage and back to the model surface. If significant temperature differences develop between the model and gage surfaces, the surface temperature step or perturbation can change the characteristics of the boundary layer, thereby changing the convective or aerodynamic heating mechanism and invalidating test results (Refs. 10 and 11). Because of good results in previous tests with 10-mil, 1/4-in.-diam thermopile Gardon gages, it was arbitrarily decided that the surface temperature of the new transducer should not exceed that of the Gardon gage.

Maximum Continuous Service Temperature — The maximum continuous service temperature of the new transducer should be at least 600°F. A transducer which can effectively operate at this temperature level should be satisfactory for the majority of continuous wind tunnel applications.

Calibration Sensitivity — The sensitivity of the transducer calibration scale factor to ambient temperature should be no worse than that of a conventional (one differential thermocouple) Gardon gage which is ≤ 5 percent deviation up to 600°F (Ref. 12).

Physical Size — The standard size of the new transducer should be 0.250 or 0.187 in. diam.

Contourability — The new transducer should be contourable. For some wind tunnel tests in the past, the surface mismatch between the model or test article and the heat gage (usually a form of Gardon gage) has produced significant data scattering because of the local forward and aft facing steps produced by these mismatches. Therefore, the surface contourability capability would be a significant improvement in the development of a heat gage for aerodynamic test requirements.

Durability — One of the most critical requirements of the new transducer is a need for improved durability. The transducer should be nearly indestructible in normal measurement applications and reusable in numerous heat transfer tests.

2.3 BASIC CONSTRUCTION

A finished 1/4-in.-diam Schmidt-Boelter gage designed for VKF continuous wind tunnel heat transfer measurement applications is shown in Fig. 3. Construction details of the gage are shown in Fig. 4. The heat flux sensing mechanism is a temperature gradient developed between the front and back plane surfaces of a 0.025-in.-thick anodized aluminum wafer or slab. A small (0.002-in.-diam) constantan wire wound around the wafer and copper-plated over one-half of the wafer in either transaxial direction (top and bottom) to form a copper-constantan series thermocouple (thermopile) as illustrated in Fig. 4 is used to measure the temperature gradient. The heat flux sensitivity of the gage is directly proportional to the number of turns of constantan wire wound around the wafer (see Fig. 5). A major breakthrough in gage construction was achieved with the use of the anodized aluminum wafer as a bobbin on which the constantan wire is wound. The aluminum wafer has a high thermal conductivity, thus permitting a fast time response, but the thin ($\leq$ 0.0005-in.) anodized layer provides electrical insulation required in winding the bare constantan wire on the wafer. A thermocouple which provides an absolute timewise temperature measurement close to the back surface of the wafer is included within the gage. Anodized aluminum is also used as the heat sink material (see Figs. 4 and 5). The potting is a thin, hard epoxy with a relatively high thermal conductivity. The nominal heat flux sensitivity of the gage is 1.5 to 3.5 mv/Btu/ft²-sec and is dependent upon the thermal conductivity of the surface epoxy (see Secs. 3.2.2.3 and 4.1.1) and the number of turns of constantan wire. The time response is $\leq$ 1.0 sec to 95 percent of full scale output and the maximum continuous service temperature of the gage is 600°F. Contouring the surface of the gage is possible, especially in a direction perpendicular to the longitudinal axis of the wafer. The gage is a very rugged device and should be almost indestructible in normal wind tunnel applications.
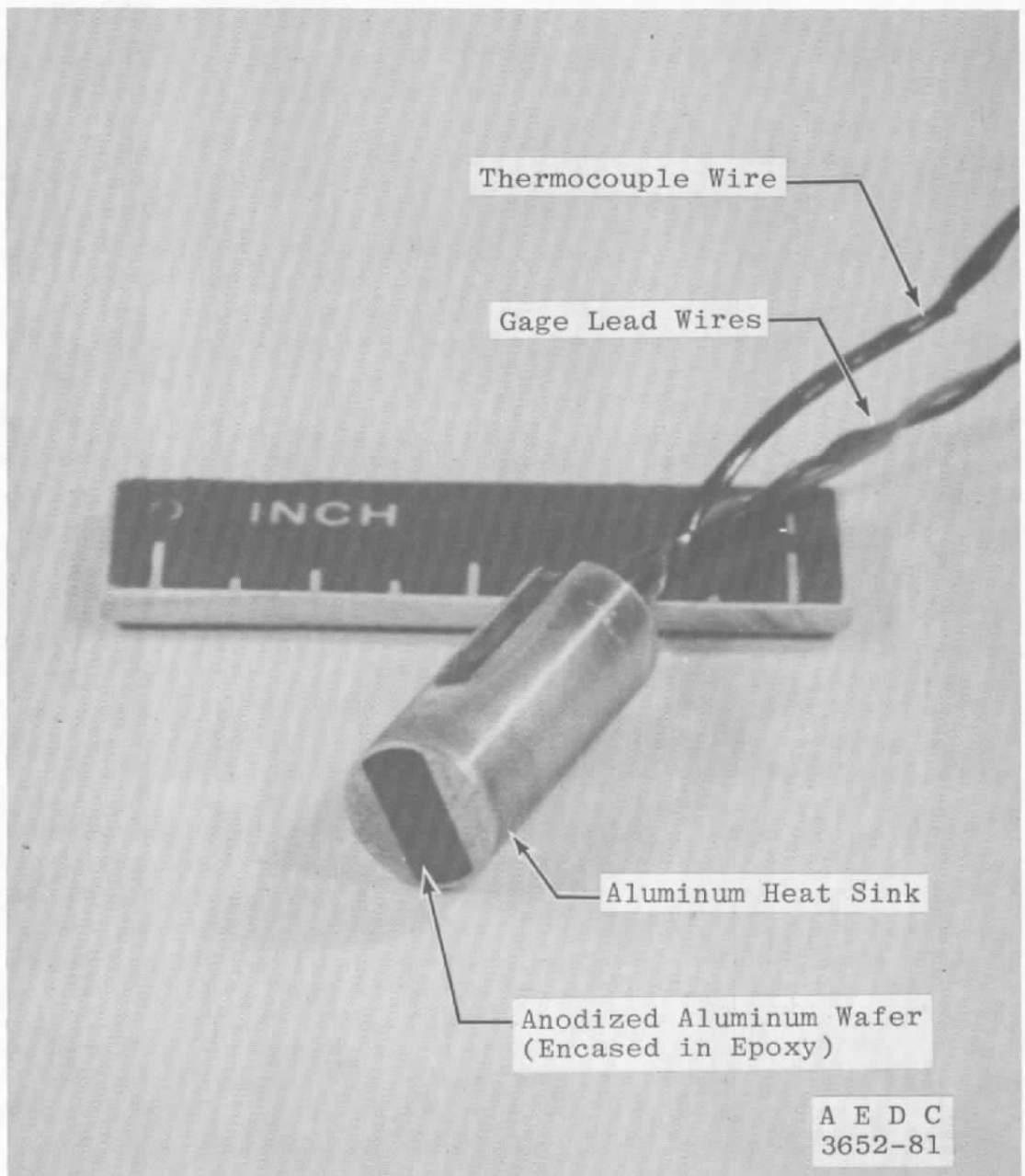
Figure 3. 1/4-in.-diam Schmidt-Boelter gage.

35 - 40 Turns 0.002-in.-diam Constantan
Wire. Electroplate Copper onto One-Half
of Coil, Both Sides (Top and Bottom)

Anodized Aluminum Wafer

Epoxy

0.003 - 0.007

0.250 OD

0.025

0.002-in.-diam
Constantan Wire.
Both Ends of
Wafer

Copper Tubing
Solder Post

Anodized
Aluminum
Heat Sink

Solder

Epoxy

A   A

0.60¹

Anodized
Aluminum
Heat Sink
0.25 OD

Top View
All Dimensions in Inches

#30 AWG Teflon
Coated Fe-Cn
(ISA Type J)
TC Wire

Epoxy

#32 AWG (7/40)
Teflon Coated
Copper Lead Wires

Section A-A

Figure 4. Section drawing of Schmidt-Boelter gage.

14

0.002-in.-diam
Constantan Wires

*Unwound End of Wafer Is
Cut Off after Winding
Constantan Coil and
Electroplating

Anodized Aluminum Heat Sink
(0.25 in. diam by 0.60 in.)

Anodized Aluminum Wafer
(0.20* by 0.09 by 0.025 in.)

A E D C
4559-81

Figure 5.   1/4-in.-diam Schmidt-Boelter gage components.

3.0 ANALYSIS

Having already described the principle of operation, design criteria, and basic construction of a prototype Schmidt-Boelter gage, the next step in the development of this measurement concept is analysis. A good understanding of gage behavior is essential to the proper application of this concept in wind tunnel aerodynamic heating measurements. This should include a knowledge or awareness of factors which affect heat flux sensitivity and time response; axial and radial temperature distributions within the gage; and effects of variations of the physical dimensions and the materials of gage components. This required knowledge of gage behavior characteristics can be attained through the application of appropriate analytical techniques. As the remainder of this section shows, analytical methods were effectively and extensively utilized in the design of the Schmidt-Boelter gage described in Sec. 2.3.

Because of its rather complex geometrical configuration, multiple material composition, and numerous heat conduction paths, the Schmidt-Boelter gage does not lend itself easily to analysis by familiar mathematical models to simulate the temperature distributions in an actual gage. Simplifying assumptions must be made to reduce the gage to a one- or two-component system for thermal analysis with exact mathematical solutions. Results of the exact solutions are helpful in pointing out general behavior patterns of Schmidt-Boelter gage performance factors such as heat flux sensitivity, time response, and surface temperature rise. However, in real world situations, the actual gage performance factors are significantly different from those obtained from the exact solution results. This is true primarily because of poor thermal contact at material surfaces, introduction of epoxies and/or adhesives, and combinations of materials wit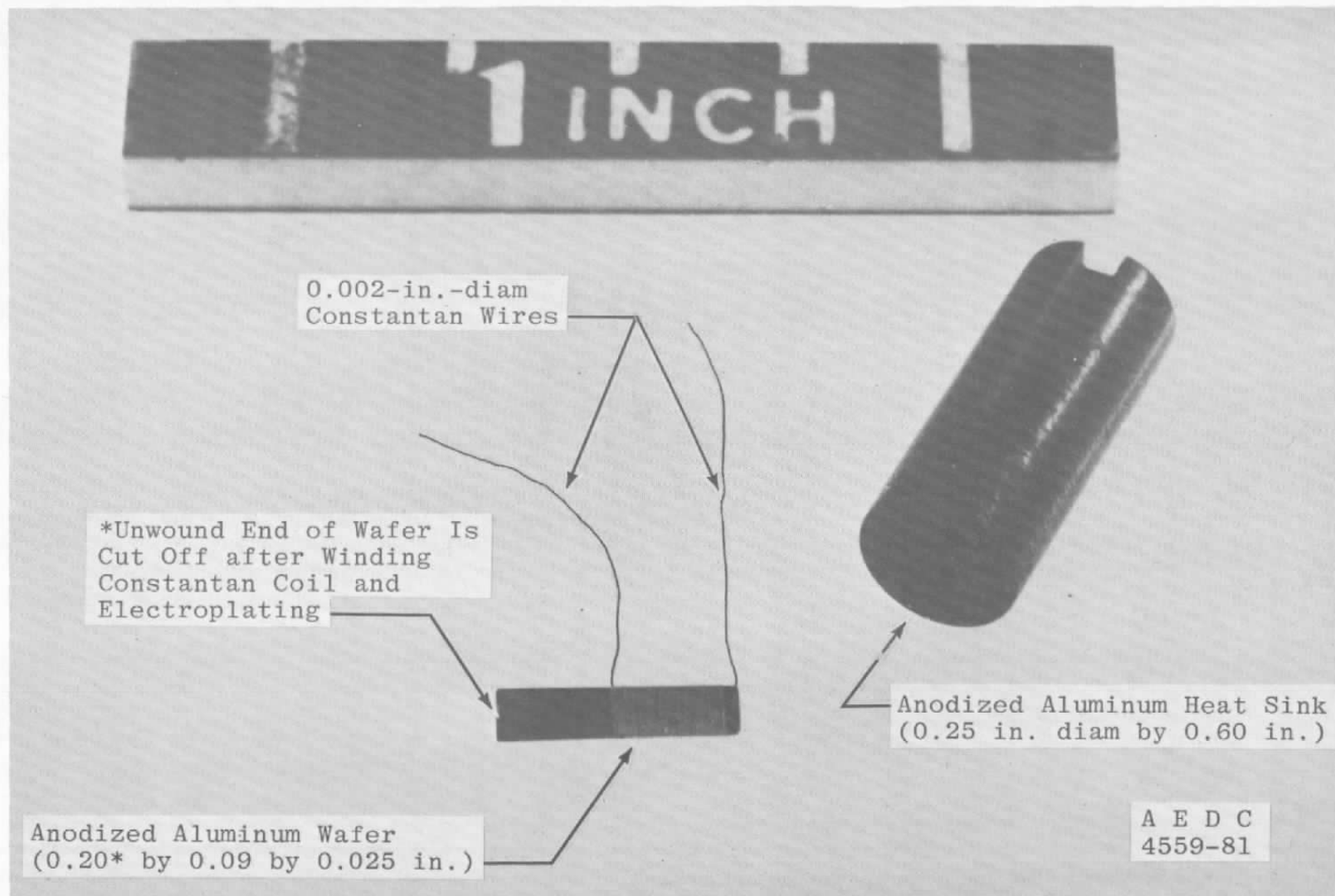h relatively high and low thermal conductivities. Therefore, another analytical method is needed to accurately predict gage behavior. One such method which was successfully used in this application is a finite-element, two-dimensional heat conduction code called TRAX (Ref. 8). The practical implementation of this analytical method has permitted accurate analysis of gage behavior for design purposes. A mathematical model which is commonly used (Refs. 5 and 7) to simulate Schmidt-Boelter gage behavior will be briefly discussed. The majority of the analysis of Schmidt-Boelter gage behavior in this report will involve application of the finite-element heat conduction code, TRAX.

3.1 MATHEMATICAL MODEL SOLUTIONS

A mathematical model used to simulate a Schmidt-Boelter gage and for which exact solutions are available is the parallel wall slab backed by a semi-infinite solid. The geometric concept of this math model is represented by Fig. 6. Exact solutions for the transient

temperature history at any axial station on or into the parallel wall slab are readily available in several heat conduction texts and reports (Refs. 13, 14, and 15). These temperature histories and combinations of temperature difference histories at various axial stations are easily programmed for repetitive calculations on a digital computer.
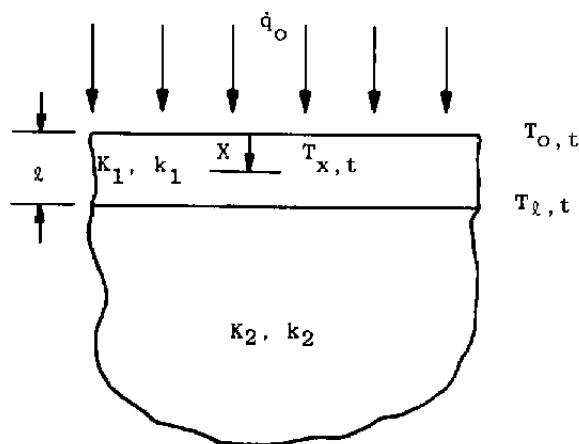
Figure 6. Parallel wall slab backed by a semi-infinite solid.

There are assumptions which must be made to make performance factor calculations using exact solutions. The gage is assumed to have only two components — a parallel wall slab and a backing material (heat sink). These two components may be any two materials. The Schmidt-Boelter gage shown in Fig. 4 has an anodized aluminum wafer (parallel wall slab) and an anodized aluminum heat sink (semi-infinite solid). Therefore, it is assumed that both components are aluminum.

Heat flux sensitivity is determined by first calculating the temperature difference between the top and bottom surfaces of the parallel wall slab (see Fig. 6). The steady-state solution to this problem is given by:

$$\Delta T = \dot{q}_o \cdot \ell/K_1 \tag{4}$$

where K_1 is the thermal conductivity of the slab and $\dot{q}_o$ is the heat flux input. Derivation of Eq. (4) is given in Appendix A. Heat flux sensitivity is given by the following expression:

$$\Delta E_o/\dot{q}_o = \ell \cdot \delta \cdot N/K_1 \tag{5}$$

It is obvious from Eq. (5) that heat flux sensitivity is directly proportional to slab thickness and inversely proportional to slab thermal conductivity.

Considering a 0.025-in.-thick aluminum wafer with 35 differential copper-constantan thermocouple junctions, a heat flux sensitivity of 0.05 mv/Btu/ft²-sec was obtained using Eq. (5). The actual Schmidt-Boelter gage sensitivity is between 1.5 and 3.5 mv/Btu/ft²-sec (see Sec. 4.1.1). Therefore, it is concluded that Eq. (5) does not give an accurate representation of the heat flux sensitivity of an actual Schmidt-Boelter gage. Calculations of time response and surface temperature rise using exact solutions do not deviate from the actual gage experimental values by as much as the heat flux sensitivity (factor of 30 to 70), but the values of these parameters disagree with the actual gage values by a significant amount ($\geq$ factor of five). It is further concluded that because of invalid assumptions regarding the material composition of the gage, exact solutions do not accurately represent the critical performance factors of the gage.

3.2 FINITE-ELEMENT SOLUTIONS

As mentioned in the preceding section, there are several assumptions regarding gage geometry and/or construction which are required in the analysis of gage performance by exact mathematical solutions. These assumptions primarily involve neglecting thin layers of adhesives, epoxies, etc., and lateral heat conduction. The combined effect of these assumptions renders an inaccurate representation of gage performance by exact solutions. An analytical technique which does not suffer from the limitations and inaccuracies of the exact solutions is TRAX (Ref. 8), a finite-element, two-dimensional heat conduction code. This heat conduction code is quite versatile because many combinations of materials, geometric configurations, and boundary conditions may be inserted into the computer program.

3.2.1 Analytical Model

A simple block diagram of the analytical TRAX model used to represent a 1/4-in.-diam Schmidt-Boelter gage is shown in Fig. 7. This is an axisymmetric model of radius, R, and length, X, with 308 elements and 345 nodal points. Each square block in Fig. 7 represents one element. The element designation is indicated by the large number in the center of the block. Each element block in Fig. 7 is also represented by four nodal points designated by the small numbers at each corner of the element blocks. The analytical TRAX model is so structured that changes in the thickness of epoxy layers above, below, and around the aluminum wafer can be easily accommodated. There is a considerably higher concentration of elements per actual surface area in the epoxy layers and wafer than in the aluminum heat sink. The reason for structuring the analytical model in this manner is to achieve better accuracy in the areas of greatest temperature gradient. It is a simple matter to change the physical dimensions of the wafer since it is comprised of 40 individual elements. Physical

dimensions of the axisymmetric body shown in Fig. 7 are close to the dimensions of the actual prototype Schmidt-Boelter gage shown in Fig. 4, with the exception of the thickness of the epoxy layer above the wafer. The thickness (0.007 in.) of the epoxy layer above the wafer shown in Fig. 7 represents a practical maximum value. Effects of decreasing this thickness on gage performance factors will be graphically illustrated in Sec. 3.2.2.3 of this report.
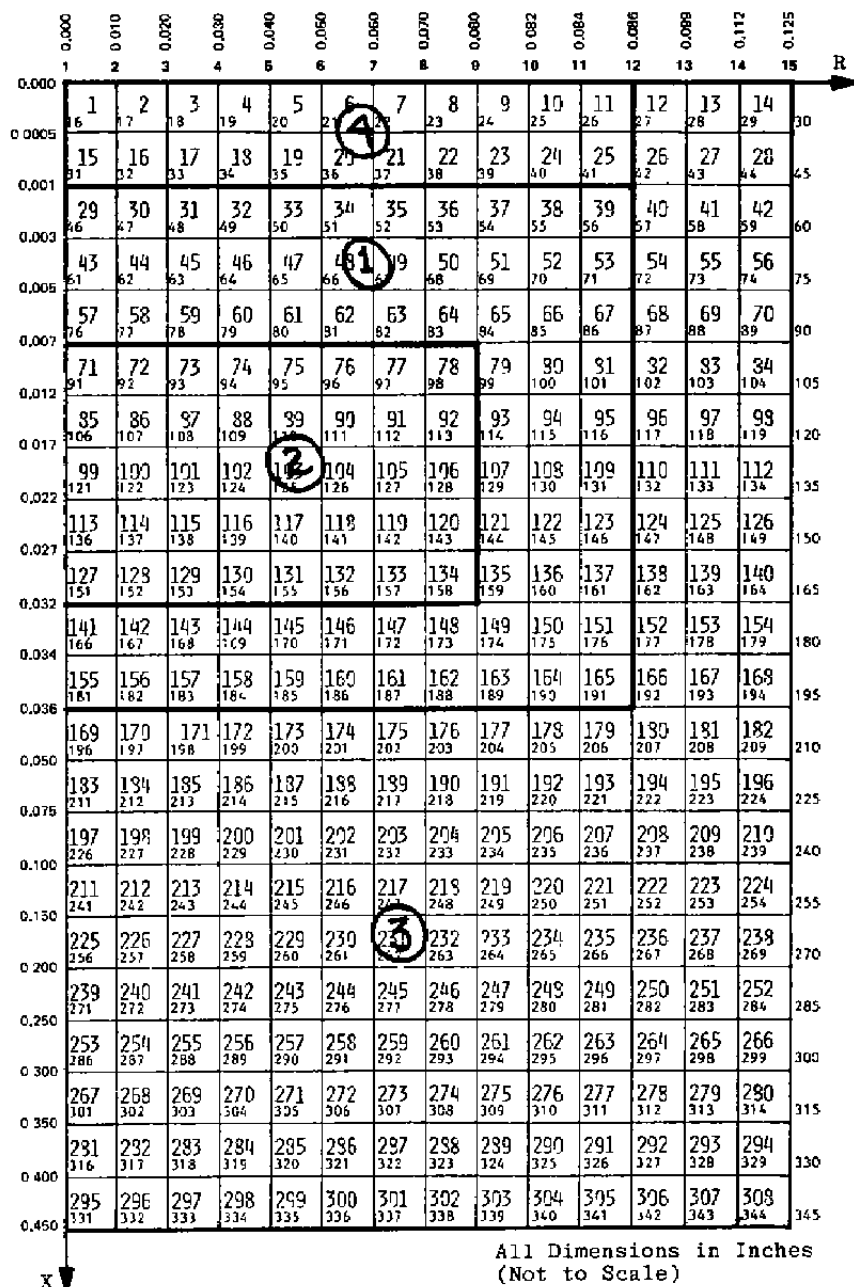

Figure 7. Block diagram of TRAX analytical model.

All Dimensions in Inches
(Not to Scale)

The analytical model is divided into four different segments which are shown separated by heavy lines in Fig. 7. Segment No. 1 represents the epoxy layers, 0.006-in.-thick on top of the wafer, 0.004-in.-thick between the bottom of the wafer and heat sink, and 0.006-in.-thick radially between the wafer and the heat sink. Segment No. 2 represents the wafer, which is a disk 0.160-in.-diam by 0.025-in.-thick. Segment No. 3 represents the heat sink which is 0.250-in.-diam by 0.45 in. with a cutout for the wafer and epoxy. Segment No. 4 represents a 0.001-in.-thick layer on the top surface of the gage which can be considered to be part of the potting. This segment can also be considered to be a low thermal conductivity adhesive which could be used to attach a surface thermocouple to the sensing surface of the gage (see Sec. 4.1.1). There were normally only two different materials considered in the structuring of the analytical model. These were aluminum for the wafer and heat sink and an epoxy. It will be shown in the following sections that the timewise temperature distributions inside the gage are influenced to a much greater degree by the thickness and thermal conductivity of the relatively thin ($\leq$ 0.007 in.) epoxies and adhesives than by the relatively thick (0.025 in.), but high thermal conductivity, wafer.

The block diagram of the analytical model (Fig. 7) is obviously not to scale. This may give some readers problems in perceiving the actual physical dimensions of gage components. If so, the reader is advised to refer to the cross-section sketch of the gage in Fig. 4.

Boundary conditions for the analysis are constant heat flux levels of 1.0 Btu/ft^2-sec at each of the 15 nodal points on the sensing surface of the gage. The thermal properties of the gage components are considered to be nontemperature dependent and the initial gage temperature is considered to be zero. The 0.002-in.-diam constantan wires wound around the anodized aluminum layers ($\leq$ 0.0005 in.) are not considered in the TRAX analysis presented in this report because preliminary results showed an insignificant effect on temperature distributions.

3.2.2 Analytical Results

The TRAX computer program calculates and prints timewise temperature data for every nodal point in the analytical model matrix at each specified print time interval. Thus, for the analytical model under consideration (345 nodal points), a large volume of tabulated data, most of which is not needed, is available to the user. This large amount of data does permit a very close examination of gage behavior and/or performance. The user can exercise engineering judgment to determine which data are of interest in his particular application. When the TRAX program is used for analysis, gage performance factors are considered collectively rather than individually. For instance, time response and heat flux sensitivity are obtained from the same group of TRAX tabulated data.

3.2.2.1 Radial Temperature Distribution

Families of curves depicting the radial temperature distribution at several different axial locations in an axisymmetric body configured as in Fig. 7 are shown in Figs. 8 and 9. The only difference in Figs. 8 and 9 is that epoxy potting materials with different thermal properties (primarily thermal conductivity — see Table 1) are considered. These data are normalized by considering a constant heat flux input of 1.0 Btu/ft^2-sec at each nodal point on the top surface of the simulated gage. The exposure time at which all data were calculated is 2.0 sec. Note the very steep temperature gradient beginning near the 0.006-in.-thick thermally insulated gap between the wafer and heat sink in the radial direction. Note also the contrast in the small temperature difference between the top and bottom surfaces of the wafer and the large temperature difference between plane surfaces just 0.002 in. above and below the wafer. Since the temperature sensor in the Schmidt-Boelter gage is basically a 0.002-in.-diam thermocouple grade constantan wire wrapped around an anodized aluminum wafer, it would seem appropriate to consider the temperature difference between the $X = 0.005$-in. and $X = 0.034$-in. axial stations as representative of the differential temperature measured in the gage. It is obvious from Figs. 8 and 9 that changes in the wafer thickness have a relatively small effect on gage behavior, but changes in potting thickness and material have a large effect. Thus, the primary heat flux sensing mechanism in the gage is the temperature gradient developed across the layers of epoxy near the constantan wire above and below the wafer. It can be surmised that the anodized aluminum wafer serves primarily as a durable, electrically insulated bobbin on which the 0.002-in.-diam constantan wire is wound.

A comparison of Figs. 8 and 9 shows there is a large difference ($>$ factor of two) in the surface temperature rise as different surface epoxies (Stycast® 3070 and Epo-Tek® 920FL) are considered. There is an even greater deviation (factor of $\cong 2.5$) between the temperature differences at axial stations $X = 0.005$ in. and $X = 0.034$ in. at radial station $R = 0.04$ in. as the same two epoxies are considered. With reference to the TRAX analytical model shown in Fig. 7, this corresponds to the calculated temperature differences between nodal points 65 and 170. The reader should note that the higher surface temperature rise and the greater temperature difference between common axial stations are realized on the gage with the lower surface epoxy thermal conductivity (see Table 1).

It was shown in Sec. 2.1.2 that it is necessary to minimize gage temperature rise when gages are used in aerodynamic heating measurement applications. Therefore, the normal practice in Schmidt-Boelter gage design is to use surface epoxies with high thermal conductivity.

Surface Temperature, T´ at X = 0.000 in.   Time = 2.0 sec

$\dot{q}_o = 1.0$ Btu/ft^2-sec

T´ at X = 0.003 in.

T´ at X = 0.005 in.

T´ at X = 0.007 in.

T´ at X = 0.032 in.

T´ at X = 0.034 in.

T´ at X = 0.036 in.

Wafer

Heat Sink

Potting in this Gap

Temperature Rise, °F

Radial Distance from Center, R, in.

0.125
0.086
0.080

0.036
0.032
0.007

$\dot{q}_o$

R

Wafer

Potting

Heat Sink

X

Materials
Wafer: Aluminum
Potting. Stycast® 3070
Heat Sink: Aluminum
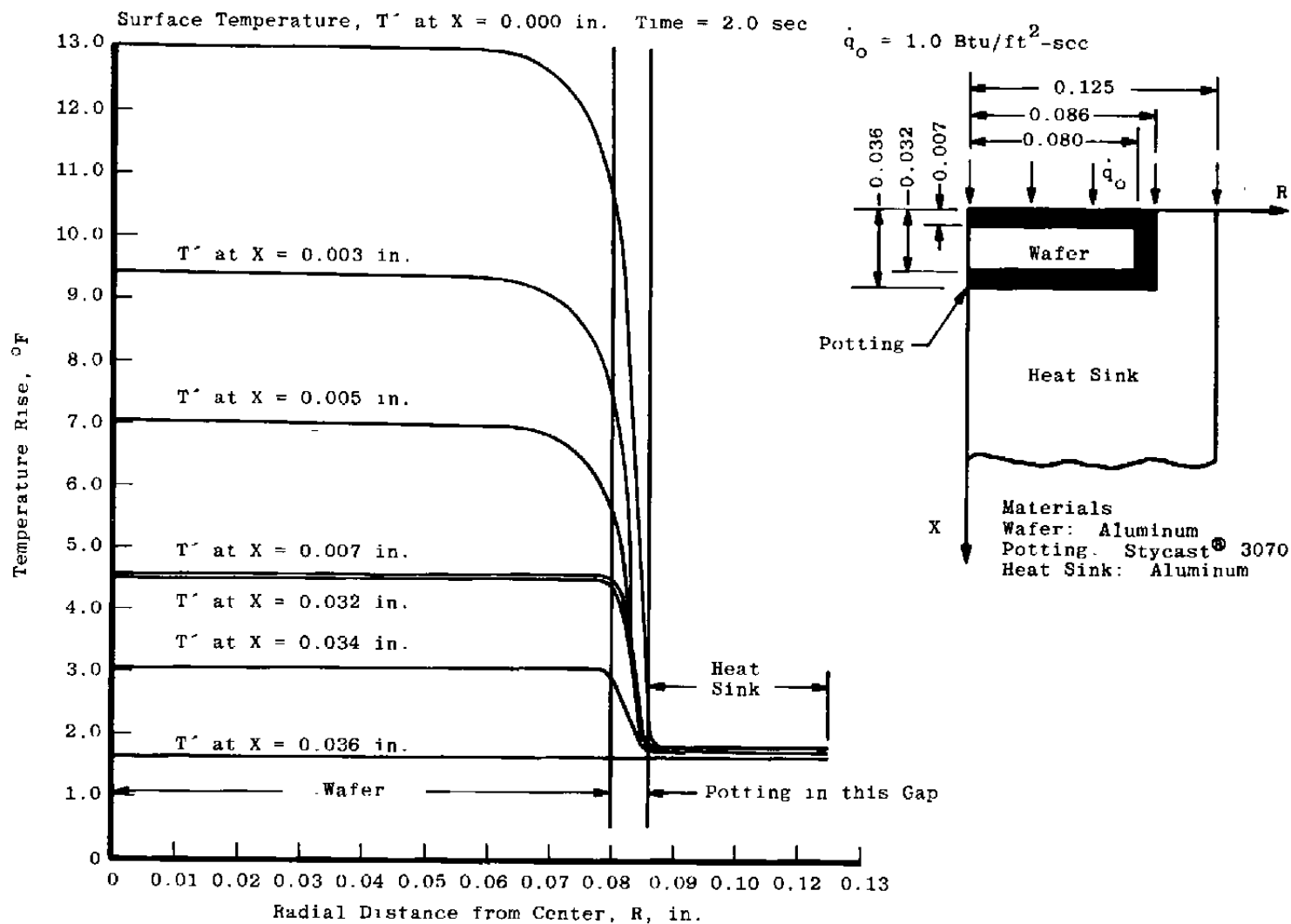
Figure 8. Radial temperature distribution in a simulated Schmidt-Boelter gage with Stycast® 3070 surface epoxy.

Temperature Rise, °F

13.0
12.0
11.0
10.0
9.0
8.0
7.0
6.0
5.0
4.0
3.0
2.0
1.0
0

Time = 2.0 sec

$\dot{q}_0$ = 1.0 Btu/ft^2-sec

Surface Temperature T´ at X = 0.000

T´ at X = 0.003 in.

T´ at X = 0.005 in.

T´ at X = 0.007 in.

T´ at X = 0 032 in.

T´ at X = 0.034 in.

T´ at X = 0.036 in.

Wafer

Heat Sink

Potting in this Gap

0   0.01 0.02 0.03 0.04 0.05 0.06 0.07 0.08 0.09 0.10 0.12 0 13

Radial Distance from Center, R, in.

0.125
0.086
0.080
0.036
0.032
0.007

$\dot{q}_0$

R

Wafer

Potting

Heat Sink

X

Materials
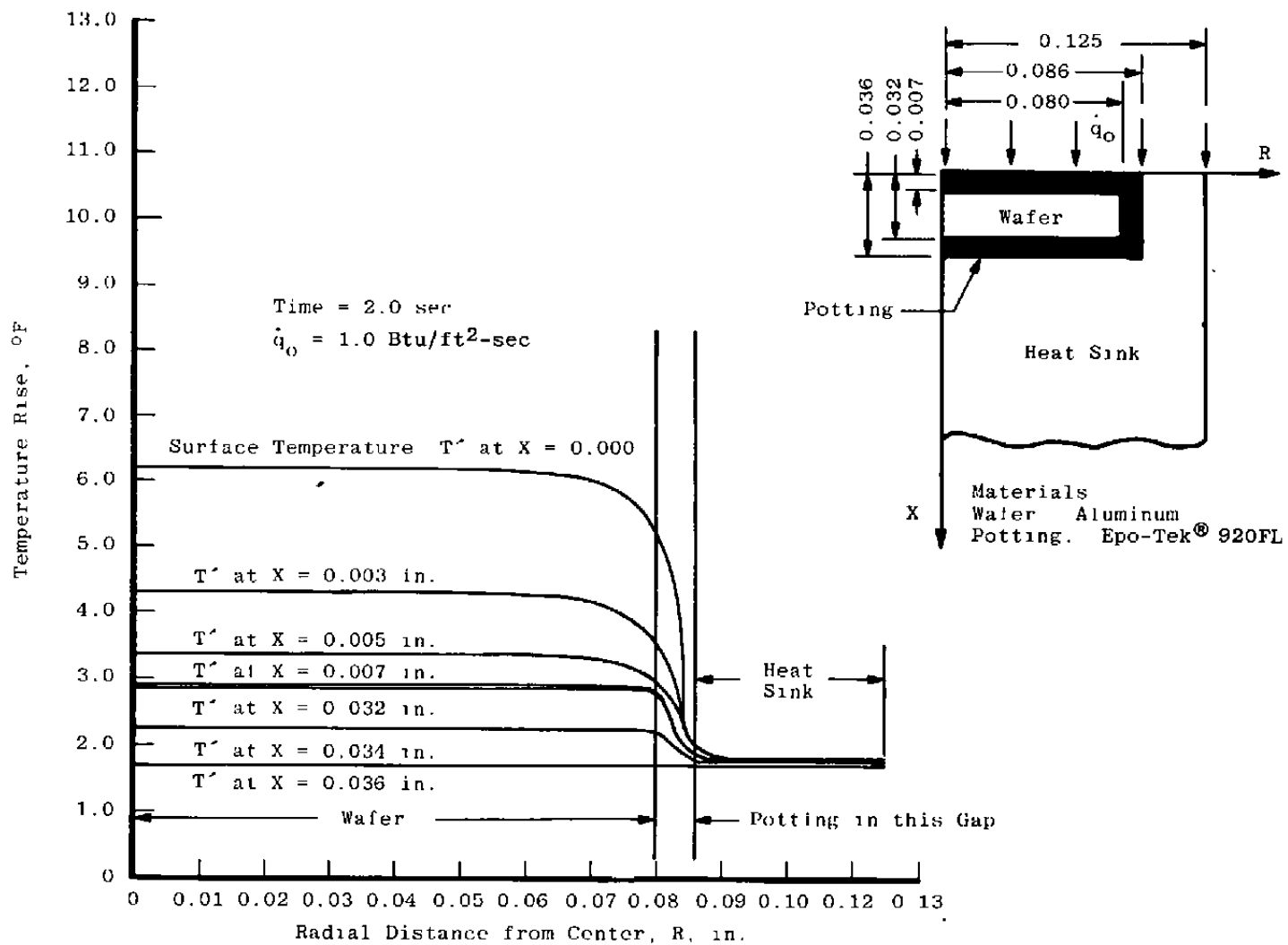Wafer   Aluminum
Potting. Epo-Tek® 920FL

Figure 9. Radial temperature distribution in a simulated Schmidt-Boelter gage with Epo-Tek® 920FL surface epoxy.

Table 1. Thermal Properties of Selected Epoxies and Adhesives

Epoxy	Maximum Service Temperature, (°F)	Thermal Conductivity, $\left(\dfrac{Btu}{in.-°F-sec}\right)$	Specific Heat*, $\left(\dfrac{Btu}{lb-°F}\right)$	Density, $\left(\dfrac{lb}{in.^3}\right)$	Comments
Stycast® 2762FT	500 - 600	17.9×10^{-6}	0.20	0.0758	Highly recommended for Schmidt-Boelter gages.
Stycast® 3070	500 - 600	5.7×10^{-6}	0.25	0.0645**	High service temperature, relatively low thermal conductivity.
Stycast® 1090	351	2.51×10^{-6}	0.30	0.0312	Low thermal conductivity epoxy, not recommended.
Epo-Tek® 920FL	400 - 500	14.6×10^{-6}	0.20	0.0803**	Highly recommended for Schmidt-Boelter gages.
Epo-Tek® H70S	572 - 752	15.4×10^{-6}	0.20	0.051	High service temperature, possible applicability.
Eastman® 910	200 - 250	4.05×10^{-6}	0.35	0.043	Low viscosity strain gage adhesive.
Aluminum Oxide	2,100	370×10^{-6}	0.20	0.133	Anodized coating.

*Estimated Value

**Measured May 4, 1981

NOTE: All values of thermal properties shown for different materials were taken from manufacturer's published data except as noted.

3.2.2.2 Axial Temperature Distribution

Figure 10 is a family of curves depicting the axial temperature distribution at several radial locations on the analytical model shown in Fig. 7, considering Epo-Tek® 920FL potting. As in Fig. 9, there is a constant heat flux on the surface of the analytical model, and the time point at which data are sampled is 2.0 sec from initial heating. Note the steep temperature gradient in the axial direction in the 0.007-in.-thick potting over the aluminum wafer. As in the preceding section, Fig. 10 shows there is a small temperature gradient across the wafer. There is another fairly steep temperature gradient in the 0.004-in.-thick potting from the bottom surface of the wafer to the heat sink. The axial temperature distribution shows no trends that were not illustrated in Fig. 9; however, the same data presented in a different graphical format may clarify gage behavior for some readers.

Figures 8, 9, and 10 graphically illustrate that large errors are incurred by neglecting thin layers of epoxies and adhesives, as was done in the exact solutions.

3.2.2.3 Performance Factors

Heat Flux Sensitivity — An analytical prediction of the heat flux sensitivity of the Schmidt-Boelter gage can be made with tabulated data from the TRAX computer program. The reader is referred to the analytical model shown in Fig. 7. A family of curves showing the radial temperature difference distributions between different parallel planes on the analytical model is shown in Fig. 11 for two different epoxies. Consider a constant heat flux of 1.0 Btu/ft²-sec at each node on the top surface. All data were calculated at a time interval of 2.0 sec after heat was first applied to the sensing surface. Selection of the proper combination of parallel planes in the analytical model as being representative of the measurement planes in an actual gage involves an arbitrary decision. For the case under consideration, the basic differential temperature sensor in the gage is a 0.002-in.-diam constantan wire wrapped around a 0.025-in.-thick anodized aluminum wafer. If the wires are considered to be fairly tightly wrapped around the wafer, the planes of measurement can be considered to be at the midpoint of the wires; i.e., $X_1 = 0.005$ in. and $X_2 = 0.034$ in. This is allowing 0.001 in. on either side of the wafer for the thickness of the anodized layer and slightly imperfect physical contact between wire and wafer. Figure 11 show that the normalized temperature difference is about 3.9°F/Btu/ft²-sec for Stycast 3070 and about 1.57°F/Btu/ft²-sec for Epo-Tek 920FL. The ratio of normalized temperature differences is very close to the reciprocal of the ratios of thermal conductivities for the two materials (see Table 1). Of course, considering measurement planes farther away from the

top surface of the aluminum wafer and closer to the sensing surface will result in higher normalized temperature differences for both materials (see Fig. 11). To convert the normalized differential temperatures into heat flux sensitivity, the number of turns of wire around the wafer and the thermoelectric sensitivity of the copper-constantan thermocouple must be considered as follows:

$$\Delta E_o / \dot{q}_o = \Delta T \cdot N \cdot \delta / \dot{q}_o \qquad (6)$$

where N is number of turns of constantan wire and δ is the thermoelectric sensitivity of a copper-constantan (ISA type T) thermocouple at 80°F. There are $\cong$ 35 turns on the wafer for the 1/4-in.-diam gage and δ is 22.7 $\mu v/°F$. Thus, the heat flux sensitivity of a simulated Schmidt-Boelter gage with Stycast 3070 potting can be written:

$$\frac{\Delta E_o}{\dot{q}_o} = \frac{3.9°F \cdot 35 \cdot 22.7 \times 10^{-3} \text{ mv}}{1.0 \text{ Btu/ft}^2\text{-sec °F}} = 3.10 \frac{\text{mv}}{\text{Btu/ft}^2\text{-sec}}$$

The heat flux sensitivity of a simulated Schmidt-Boelter gage with Epo-Tek 920FL potting can be written:

$$\frac{\Delta E_o}{\dot{q}_o} = \frac{1.57°F \cdot 35 \cdot 22.7 \times 10^{-3} \text{ mv}}{1.0 \text{ Btu/ft}^2\text{-sec °F}} = 1.25 \frac{\text{mv}}{\text{Btu/ft}^2\text{-sec}}$$

The section on experimental laboratory evaluation will show that these values of estimated heat flux sensitivity are well within the range of sensitivities of actual gages.

Another important and attractive feature of the Schmidt-Boelter gage with regard to heat flux sensitivity can be illustrated with the aid of the TRAX computer program. This feature involves a minimal change in heat flux sensitivity as layers of potting are removed from the sensing surface of the transducer above the wafer. The reader is again referred to Fig. 7. Consider removing a 0.002-in.-thick layer of potting from the analytical model. This involves changing the axial (X direction) dimensions of the model. Now the new planes of measurement are $X'_1 = 0.003$ in. and $X'_2 = 0.032$ in. Figure 11 shows the normalized temperature difference for the measurement planes at X'_1 and X'_2 for the two epoxies under consideration. The normalized temperature difference, which is proportional to heat flux sensitivity, changed from 3.90 to 3.98°F/Btu/ft²-sec and from 1.57 to 1.60°F/Btu/ft²-sec for Stycast 3070 and Epo-Tek 920FL epoxies, respectively. This represents a change in heat flux sensitivity of about two percent in each case. In practical cases, moderate contouring of Schmidt-Boeler gages in models should be possible without significantly affecting the gage calibration.
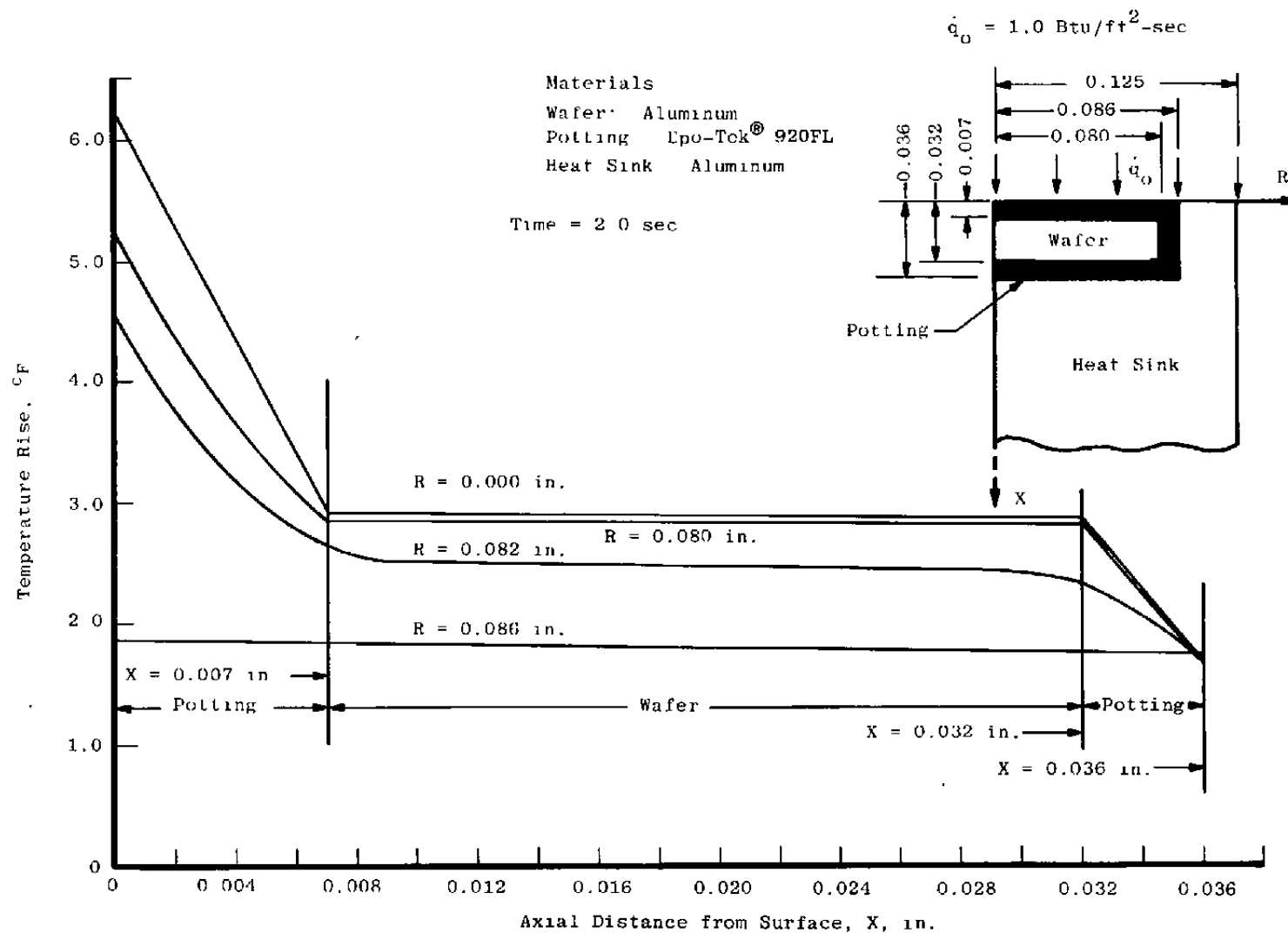
Figure 10. Axial temperature distribution in a simulated Schmidt-Boelter gage with Epo-Tek® 920FL surface epoxy.

Time = 2.0 sec $\dot{q}_o$ = 1.0 Btu/ft^2-sec

X$_1$ = 0.003 in., X$_2$ = 0.034 in., Stycast® 3070

X$_1'$ = 0.003 in., X$_2'$ = 0.032 in., Stycast® 3070

X$_1$ = 0.005 in., X$_2$ = 0.034 in.; Stycast® 3070

X$_1$ = 0.003 in., X$_2$ = 0.034 in.; Epo-Tek® 920FL

X$_1'$ = 0.003 in., X$_2'$ = 0.032 in., Epo-Tek® 920FL

X$_1$ = 0.005 in., X$_2$ = 0.034 in., Epo-Tek® 920FL

Potting in this Gap

Normalized Temperature Difference, °F/Btu/ft^2-sec

6.0
5.0
4.0
3.0
2.0
1.0
0

0   0.01   0.02   0.03   0.04   0.05   0.06   0.07   0.08   0.09

Radial Distance, R, from Centerline of Axisymmetric Body, in.

X$_2$ X$_1$ $\dot{q}_o$ 0.007 0.032 0.036

R

Wafer

Potting

Heat Sink

X

28

Figure 11. Normalized radial differential temperature distribution in an axisynmetric body.

Time Response — An analytical prediction of Schmidt-Boelter gage time response can also be made from the TRAX computer program timewise tabulated data. Again the reader is referred to the block representation of the analytical model shown in Fig. 7. Normalized time response data are obtained by dividing the timewise differential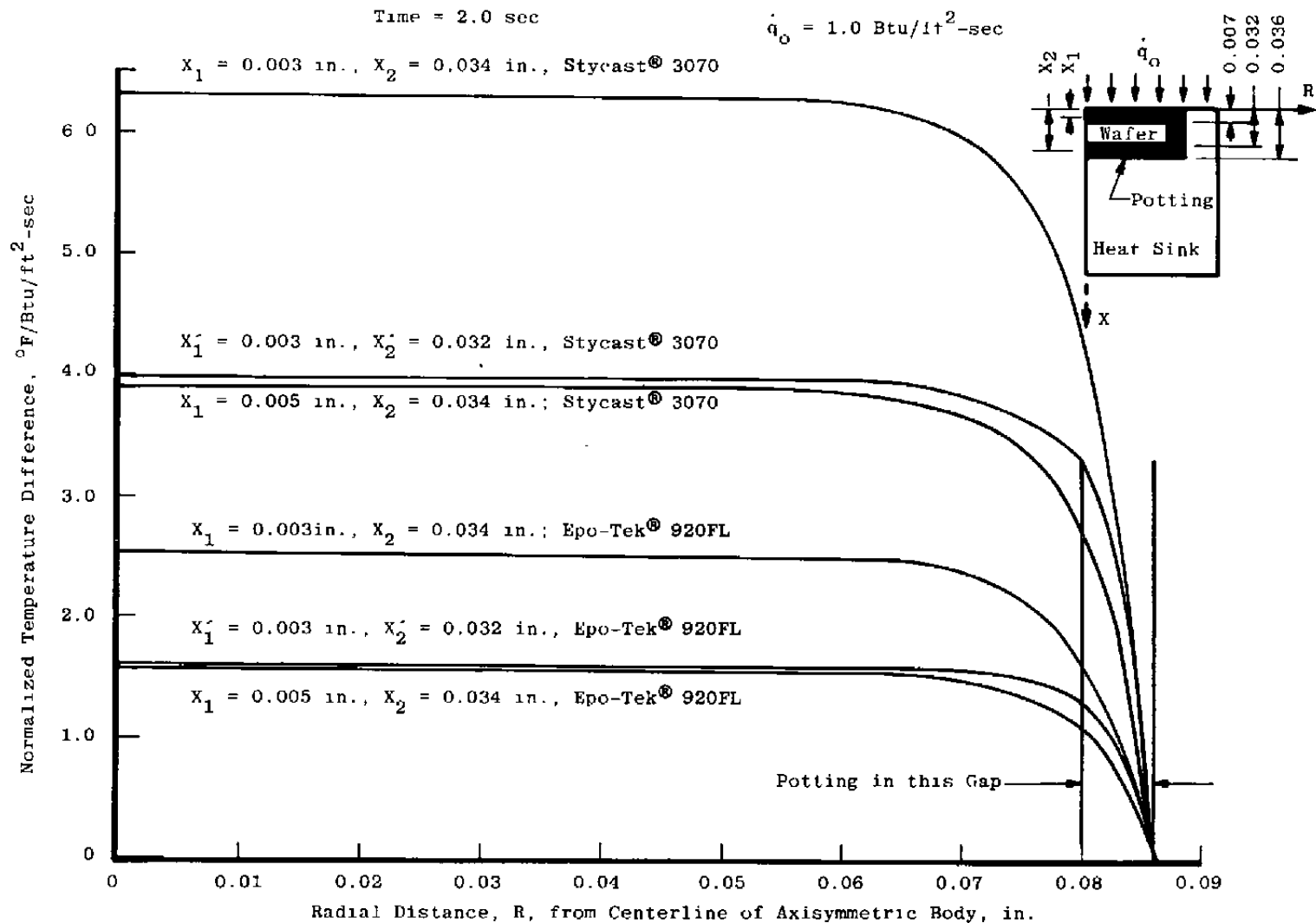 temperature between a selected pair of nodal points on either side of the aluminum wafer by the asymptotic value. In order to maintain consistency, only nodal points located on the axial centerline ($R = 0$ in.) of the axisymmetric body were considered. Graphical illustrations of TRAX time response data for two different potting materials are shown in Fig. 12. The analytical model planes of measurement are the same as were considered in the preceding section on heat flux sensitivity; that is, $X_1 = 0.005$ in. and $X_2 = 0.034$ in. Figure 12 shows that the time response is significantly better when a material of higher thermal conductivity (Epo-Tek 920FL) is used. The effect of removing a 0.002-in.-thick layer of potting from the analytical model with Stycast 3070 potting is shown by the dashed line. With regard to structuring the analytical model, the procedure is identical with that in the preceding section. New planes of measurement are $X'_1 = 0.003$ in. and $X'_2 = 0.032$ in. A slight improvement in time response is seen.

Figure 13 shows the effect of considering different planes of measurement above the aluminum wafer on the time response of the Schmidt-Boelter gage. The analytical model is the modified version of Fig. 7 with the top 0.002 in. of potting removed. As expected, the graphical illustrations show the time response is better (faster) when the planes of measurement closest to the surface of the gage are considered.

Surface Temperature Rise — Because of various aerodynamic effects, knowledge of the surface temperature of a gage or sensor is necessary for accurate heat transfer measurements in continuous wind tunnel applications (see Sec. 2.1.2). However, the mere knowledge of surface temperature cannot, in itself, ensure accurate measurements. Rather, the surface temperature rise of a gage must be controlled within acceptable limits. The gage surface temperature must reside at or near the temperature of the aerodynamic configuration on which measurements are desired. It is impractical to measure the transient surface temperature of a heat flux gage in most actual wind tunnel measurement applications. However, transient temperature can be measured inside the gage below the surface with relative ease. An analytical and/or experimental method for predicting the difference between the measured temperature and the surface temperature is necessary. The two-dimensional heat conduction code, TRAX, provides an analytical method for obtaining this result. Laboratory experimental data which complement the analytical method were obtained and will be discussed in Sec. 4.1.1.
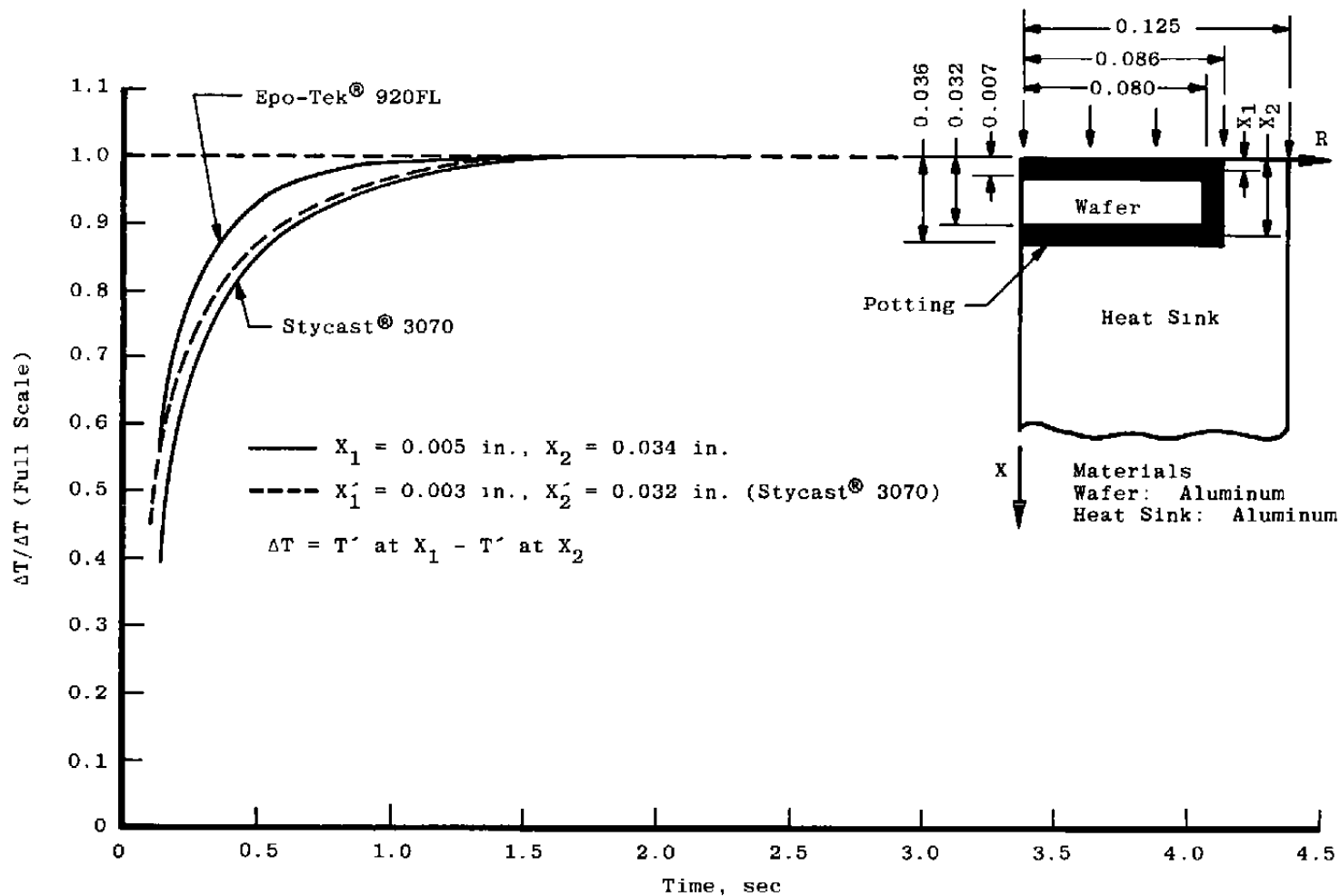
Figure 12. Normalized time response of Schmidt-Boelter gages with different surface epoxies.
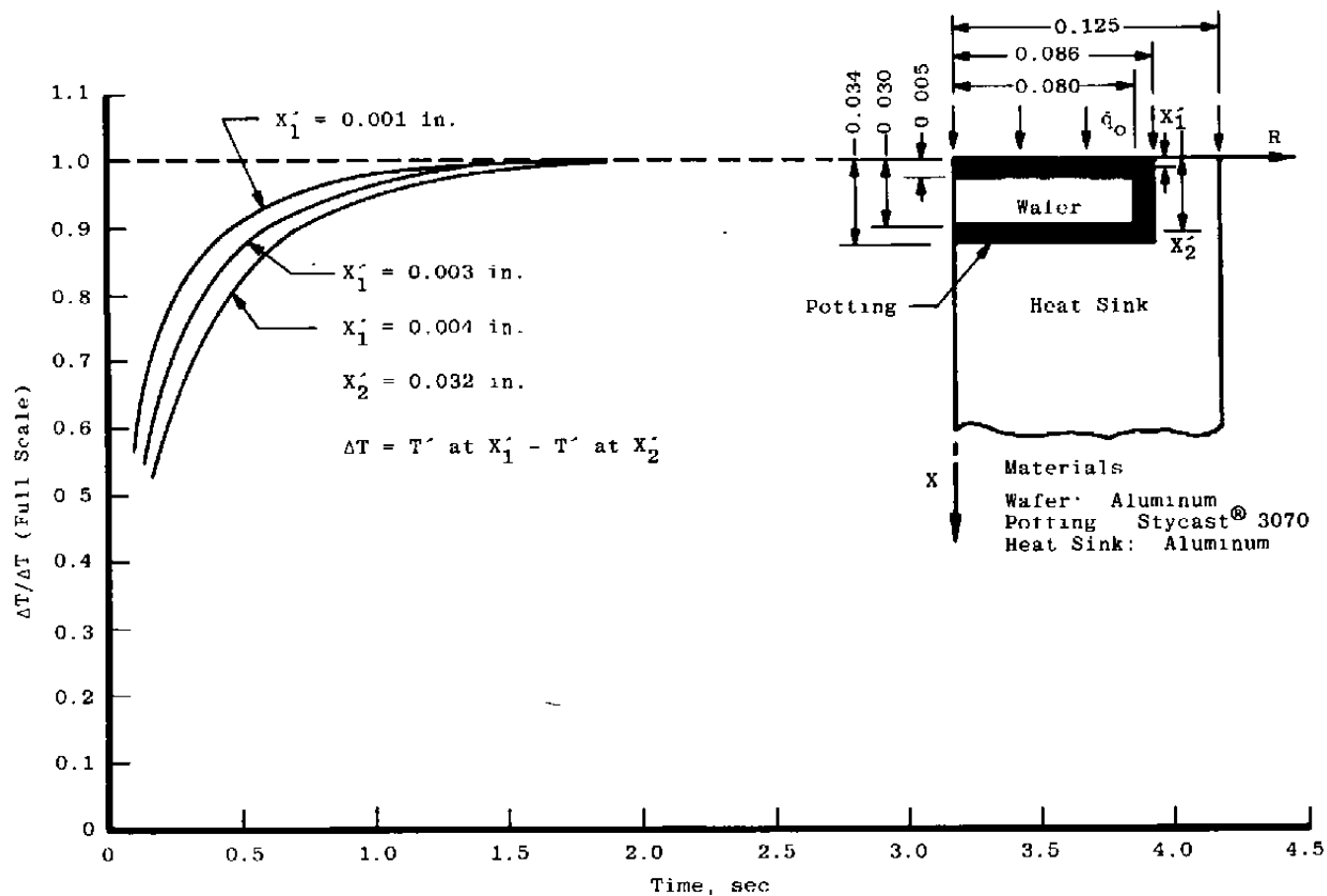
Figure 13. Effect of surface epoxy thickness on time response of a Schmidt-Boelter gage.

Figure 14 is a graphical illustration of the analytical prediction (TRAX solution) of transient temperatures at various axial locations in a simulated Schmidt-Boelter gage. The same analytical model (see Fig. 7) used in the sections on heat flux sensitivity and time response was used in this analysis. Only axial nodal points on the radial midpoint (R = 0.040 in.) of the aluminum wafer were considered. Just as in the preceding sections, two different, but practical, potting materials were considered to dramatize the effects of variations in thermal properties on gage temperature rise. Data were normalized to a constant heat flux level of 1.0 Btu/ft^2-sec on the sensing surface for easy extrapolation to other levels.

Several important gage temperature distributions can be seen from Fig. 14. First, the transient surface temperature histories of gages with the same geometrical configurations (node 5, Fig. 7), but with different thermal properties of the potting materials (see Table 1), vary by a constant and significant amount ($\cong$ 7°F). Although there are other terms to be considered, this constant temperature difference should generally vary as does the lumped thermal parameter, $(kt/K)^{1/2}$, for the different potting materials [see Eq. (A-1), Appendix A]. The temperature histories, T_{w_2}, at the back of the wafer (node 155, Fig. 7) vary by a constant, but lesser, amount ($\cong$ 1.6°F). The temperature histories, T_{HS}, at the axial interface between potting and heat sink (node 185, Fig. 7) differ by an insignificant amount for gages with the two potting materials under consideration.

The effect of removing a 0.002-in-thick layer of potting from the surface of the gage is also shown in Fig. 14. This is identified by X'_1 = 0.005 in. for two curves representing each of the potting materials. The other temperature histories, T_{w_2} and T_{HS}, did not change by a significant amount when the 0.002-in-thick layer of potting was removed from the gage. Hence, they are not shown on Fig. 14.

From observations of plotted TRAX data on Fig. 14, it can be reasoned that Schmidt-Boelter gage temperature rise can be minimized by using thin layers of potting with high thermal conductivity. Of course, there are other considerations in gage design, and design tradeoffs are required.
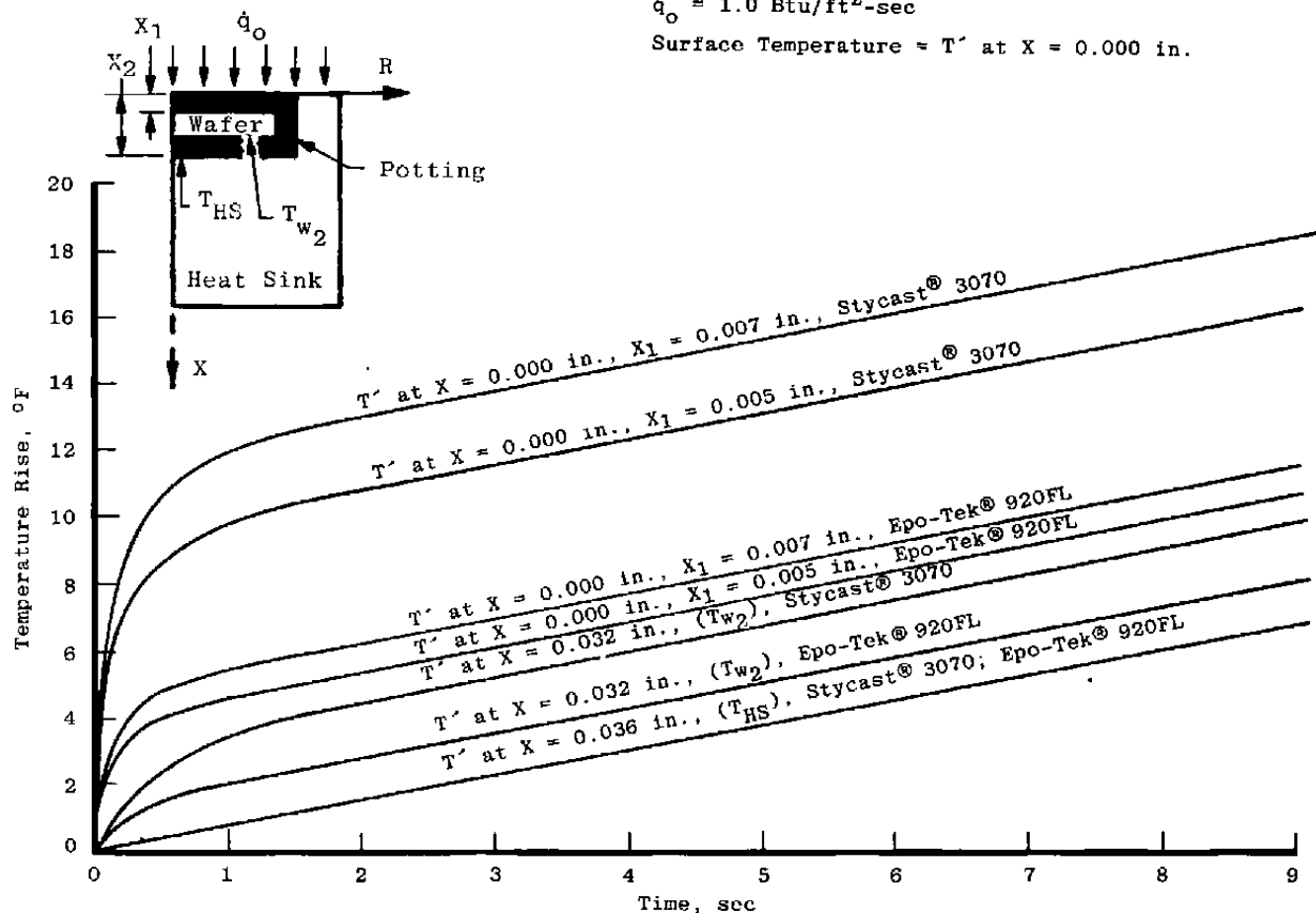
Figure 14. Transient temperature distribution in a simulated Schmidt-Boelter gage with different surface epoxies.

4.0 EXPERIMENTAL RESULTS

4.1 LABORATORY EVALUATION

Before being used in wind tunnel tests, experiments are performed on heat flux transducers in the laboratory to determine critical performance factors. This section describes experimental laboratory procedures used to determine performance factors of prototype Schmidt-Boelter gages fabricated at the AEDC/VKF.

4.1.1 Heat Flux Sensitivity

The experimental heat flux sensitivity of Schmidt-Boelter gages is determined in a simple and straightforward manner in the laboratory. This procedure basically consists of applying a known and nearly constant heat flux from a radiant heat source to the sensing surface of the transducer and measuring the output signal. This is essentially the same procedure used in the routine calibration of heat flux transducers which will be described in detail in Sec. 4.2. Table 2 shows the experimental sensitivities of several prototype Schmidt-Boelter gages at room temperature ambient temperature conditions. It is obvious that there is a relatively wide variation in the experimental sensitivities of some of the prototype gages. In general, the gages potted with Epo-Tek 920FL have lower heat flux sensitivities than the gages potted with Stycast 3070. From the TRAX analytical predictions in Sec. 3.2.2.3, this trend is anticipated. There is good general agreement with the experimental sensitivities shown in Table 2 and TRAX predictions. There are variations in the heat flux sensitivities within a group of gages potted with the same epoxy. These variations are probably caused by inconsistencies in the fabrication procedure for each gage. Differences in the effective distance between planes of differential temperature measurement within the potting and number of turns of constantan wire are possible sources of variance.

4.1.2 Experimental Time Response

Having previously metioned the difficulties in predicting the time response of an actual Schmidt-Boelter gage by analytical means, the determination of transducer time response by experimental methods will be discussed in this section. Basically, the experimental method involves irradiating the sensing surface of a transducer with a constant heat flux input while simultaneously monitoring the timewise transducer output. One word of caution is in order at this point. The heat source should produce a constant heat flux over the time period of interest. Otherwise, the time response data will be difficult to evaluate. Common laboratory heat sources such as quartz tube lamp banks are not suitable for this experiment because the heat flux continues to rise somewhat even after a 60-sec warmup period. A motion picture

projection lamp was chosen as the radiant heat source because of its fast rise to a constant heat flux level. A photocell was used in these experiments to indicate the time response of the heat source.

Table 2. Experimental Heat Flux Sensitivities of Prototype Schmidt-Boelter Gages

Gage Serial Number	Experimental Heat Flux Sensitivity, $\dfrac{mv}{Btu/ft^2\text{-}sec}$	Surface Potting Material
SB-3	0.826	Epo-Tek® 920FL
SB-4	1.20	
SB-5	1.14	
SB-6	1.58	
SB-7	1.08	
SB-8	1.56	
SB-9	1.24	
SB-10	2.79	Stycast® 3070
SB-11	3.25	
SB-12	2.64	
SB-13	3.15	
SB-14	2.21	
SB-15	1.52	
SB-16	3.45	
SB-17	2.63	
SB-18	2.22	
SB-19	2.82	

The apparatus used in the time response experiments is shown schematically in Fig. 15. The Schmidt-Boelter gage and photocell were located side-by-side or in the same position relative to the heat source. A fast-acting mechanical shutter was placed between the heat source and the plane surface of the transducer/photocell. Electrical power was applied to the motion picture projection lamp. After a brief warmup period (about 10 sec) the mechanical shutter was actuated, simultaneously irradiating the sensing surfaces of the transducer and photocell. A timewise record of the outputs of both the photocell and transducer is shown graphically in Fig. 16. The photocell output responds instantaneously, whereas the Schmidt-Boelter gage output approaches an asymptotic value more slowly. The photocell output thus provides a reference point from which the time response of the Schmidt-Boelter gage can be accurately determined.
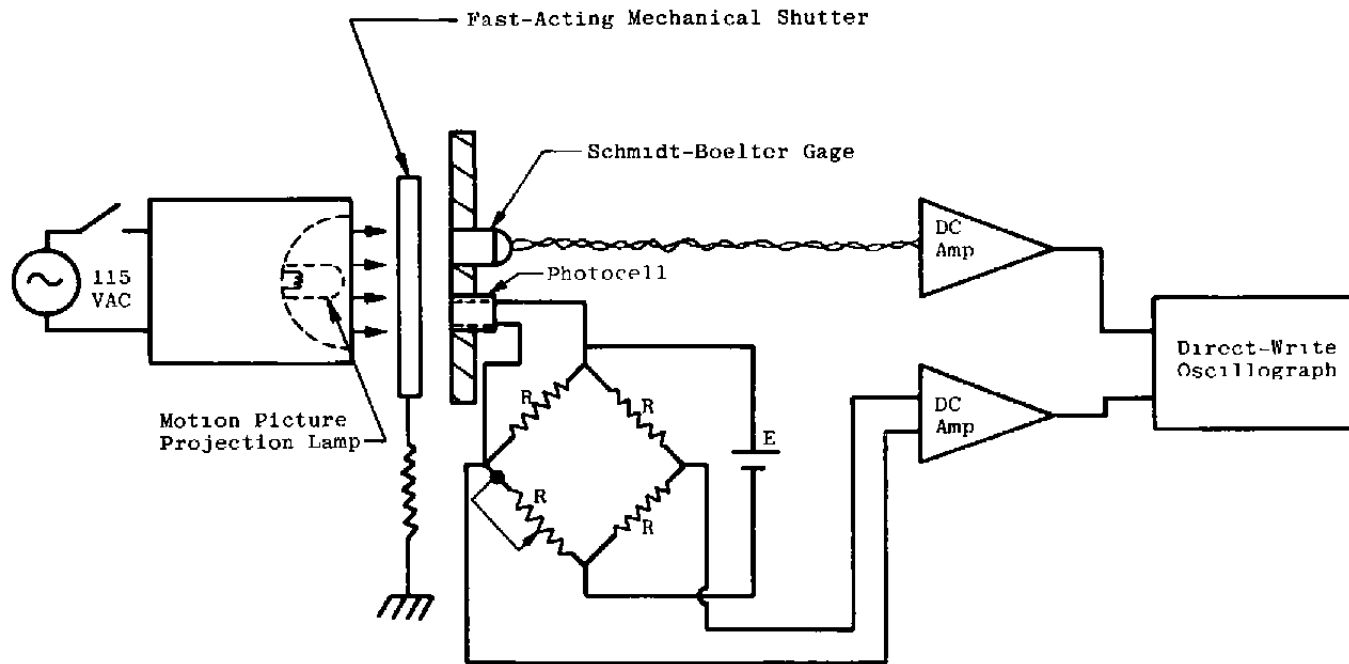
Figure 15. Schematic diagram of experimental time response apparatus.
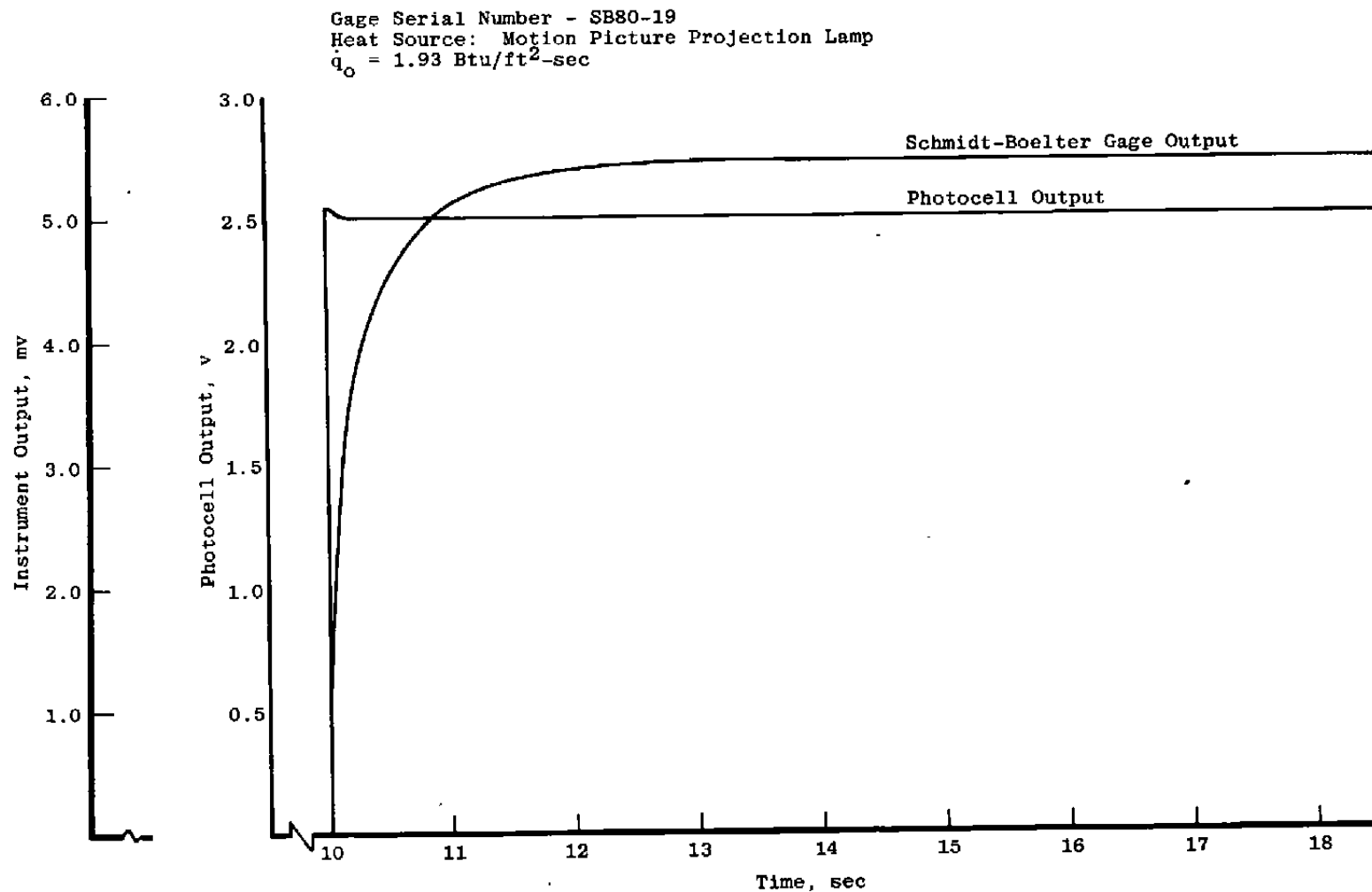
Figure 16. Schmidt-Boelter gage experimental time response data.

Normalized time response records of three Schmidt-Boelter gages are shown in Fig. 17 for gages fabricated with two different surface epoxies. Note the data from the two gages with Stycast 3070 surface epoxy (full line) are nearly coincident, indicating almost perfect agreement. Data from the gage with Epo-Tek 920FL surface epoxy (dashed line) represent a faster time response. Time response to 95 percent of full scale is about 0.70 sec for the gage with Epo-Tek 920FL potting, and is about 1.10 sec for the two gages with Stycast 3070 epoxy. These time response data are typical of Schmidt-Boelter gages fabricated to date and are in good agreement with TRAX analytical predictions (see Fig. 12).

4.1.3 Surface Temperature Rise

Heat flux gage surface temperature rise is an important parameter in aerodynamic heat transfer measurement applications because gage temperature is required in heat transfer coefficient calculations, and gage surface temperature determines the extent of possible model or test article surface temperature perturbation effects.

Usually it is impractical to measure the surface temperature of heat gages in wind tunnel measurements. Rather, a temperature inside the gage is measured and the surface temperature is estimated by adding a calculated temperature to the measured temperature. This procedure is applied to both Gardon and Schmidt-Boelter gages. Laboratory experiments are performed under controlled conditions to accurately predict the difference in surface and measured temperatures inside the gage for wind tunnel measurement applications. A description of experimental procedures for the measurement and calculation of heat gage surface temperatures is given in the following paragraphs.

First, a very thin (0.0002-in.) foil thermocouple was attached to the sensing surface of a Schmidt-Boelter gage with a low viscosity strain gage adhesive. An effort was made to locate the measuring junction of the thin foil thermocouple as closely as possible to the center of the sensing surface of the gage. The instrumented Schmidt-Boelter gage was placed in a copper calibration block which also contained two transfer standard gages. Both the surface thermocouple and the inside gage thermocouple lead wires were routed through appropriate cold junction compensators which simulate individual 32°F thermocouple reference junctions. Heat gage output leads and thermocouple reference junction output leads were connected to a computer-controlled multichannel data acquisition system. The sensing surfaces of the sensors were painted with a thin ($\cong$ 0.0005-in.) coating of Krylon® No. 1602 ultra-flat black spray enamel (see Sec. 4.2.2). The calibration block containing the heat gages was placed in a radiant heat flux calibration facility composed of nine 1,000-w quartz tube lamps. The gage to be tested and the transfer standard gages were simultaneously irradiated with a nearly constant and preset heat flux level of 1.0 Btu/ft²-sec. The gage and

38

thermocouple output signals were sampled at 0.10-sec time intervals over a time period of about 10 sec. This experimental procedure was performed for two prototype 1/4-in.-diam Schmidt-Boelter gages and one 10-mil, 1/4-in.-diam thermopile Gardon gage.

Graphical results of the experiments described in the preceding paragraph in the form of timewise plots of measured surface temperature rise for two Schmidt-Boelter gages and one thermopile Gardon gage are shown in Fig. 18. Also shown in Fig. 18 is a timewise plot of measured heat flux. This measured heat flux represents the average of the readings from two transfer standard gages. The input heat flux was intentionally set at 1.0 Btu/ft^2-sec to normalize the temperature data. Note the difference in surface temperature rise for Schmidt-Boelter gages SB-4 and SB-19. This is to be expected because SB-19 was potted with an epoxy (Stycast 3070) with a lower thermal conductivity than that (Epo-Tek 920FL) for gage SB-4 (see Table 1). Note also that the surface temperature rise for SB-4 and the thermopile Gardon gage was almost identical with regard to magnitude and shape. This is a desired result which should allow these gages to be used interchangeably in aerodynamic heat flux measurement applications.

Figure 19 provides a comparison of the measured timewise Schmidt-Boelter gage surface temperature and inside gage temperature with TRAX predictions for two gages with different surface epoxies. The measured data are from the two Schmidt-Boelter gages described in the preceding paragraph. One difference in the analytical data shown in Fig. 19 and other TRAX data described in Sec. 3.2.2.3 is that the top 0.001-in.-layer was considered to be Eastman® 910 adhesive (see Table 1). The 0.001-in.-thick layer of Eastman® 910 was included in the TRAX analysis because the surface thermocouples were bonded to the sensing surfaces of the Schmidt-Boelter gages with this adhesive. The remaining 0.006-in.-thick layer over the wafer was Sytcast 3070 or Epo-Tek 920FL. Also shown in Fig. 19 is a comparison of the measured inside gage temperature and a TRAX temperature history T_{HS} at nodal point No. 185 at $X = 0.036$ in. of the analytical model (see Fig. 7). Although the surface temperature histories representing the measured and analytical data shown on Fig. 19 deviate somewhat, the data agreement is quite good. For instance, the surface temperature history for the gage fabricated with Stycast 3070 epoxy agrees with TRAX predictions within 1°F at a time of 5 sec from initial application of heat. The agreement between analytical and measured data for the gage with Epo-Tek 920FL surface epoxy was about 3°F at the same time point. Although the measured surface temperature for both cases considered is higher than TRAX analytical data, the measured inside gage temperatures are slightly lower (≤ 1.1°F deviation) at a time point of 5 sec.

Based on experimental results shown in Figs. 18 and 19, Schmidt-Boelter gage surface temperature rise for continuous wind tunnel measurement applications will be calculated by

adding 10.4°F/Btu/ft²-sec to the measured inside gage temperature for a gage with Epo-Tek 920FL potting, and 13.8°F/Btu/ft²-sec for a gage with Stycast 3070 potting. The optimum Schmidt-Boelter gage design will contain a higher thermal conductivity surface epoxy than either Stycast 3070 or Epo-Tek 920FL, probably Stycast® 2762FT (see Table 1). More extensive experimental work is planned to verify the procedure for obtaining the correct gage surface temperature with different surface epoxies. The experimental procedures for performing this work should be basically as described in this section, but would involve more gages.

4.2 CALIBRATION

Routine experimental calibrations of heat flux transducers are generally performed in a radiant heating facility. This section will describe the calibration apparatus utilized, procedures followed, and results of experimental calibrations performed in conjunction with the development of the Schmidt-Boelter gage.

4.2.1 Apparatus

Although limited by physical size to the simultaneous irradiation of six 1/4-in.-diam sensors, the most versatile radiant heat flux calibration facility at the AEDC/VKF is pictured in Fig. 20. This facility is capable of supplying nearly constant incident heat flux levels up to 10 Btu/ft²-sec, and it has the additional capability of performing calibrations at elevated ambient temperatures up to 1,000°F. This facility was used to calibrate the majority of the heat flux gages referred to in this report. The heat source is a Model 4083 Pyropanel® modular infrared radiant heater manufactured by Research Inc. The 4083 Pyropanel contains six equally-spaced (1.0-in.-centerline) 500-w, tungsten filament, quartz envelope lamps (0.40-in.-diam by 8.5 in.). The heating lamps used in the Pyropanel unit attain a temperature of approximately 4,000°F at rated voltage (120 VAC). Ceramic (silica) reflectors provide a diffusely reflecting background for the unit.

Gages to be calibrated are installed in a stainless steel gage support block (3.5-by 1.0-by 1.0-in.) which conveniently slides into a cavity in a larger mounting assembly block (5.0-by 2.5-by 2.5-in.). The mounting assembly block is secured to Unislide® assemblies which provide vertical and horizontal movement of the gages relative to the heat source (see Fig. 20). A longitudinal heat flux map of the calibration facility at a vertical distance of 2.1 in. between the heat source and the top surface of the gage support block is shown in Fig. 21. There are three 250-w electrical strip heaters (4.5-by 1.5-by 0.375-in.), one on each longitudinal side and one on the bottom, attached to the mounting assembly block to provide heating for elevated temperature heat gage calibrations. A digital indicating temperature controller is used in conjunction with the elevated temperature calibrations.

41

Heat Source· Motion Picture Projection Lamp

Symbol	Gage Serial Number	Surface Epoxy
----	SB-4	Epo-Tek® 920FL
——	SB-10, SB-19	Stycast® 3070
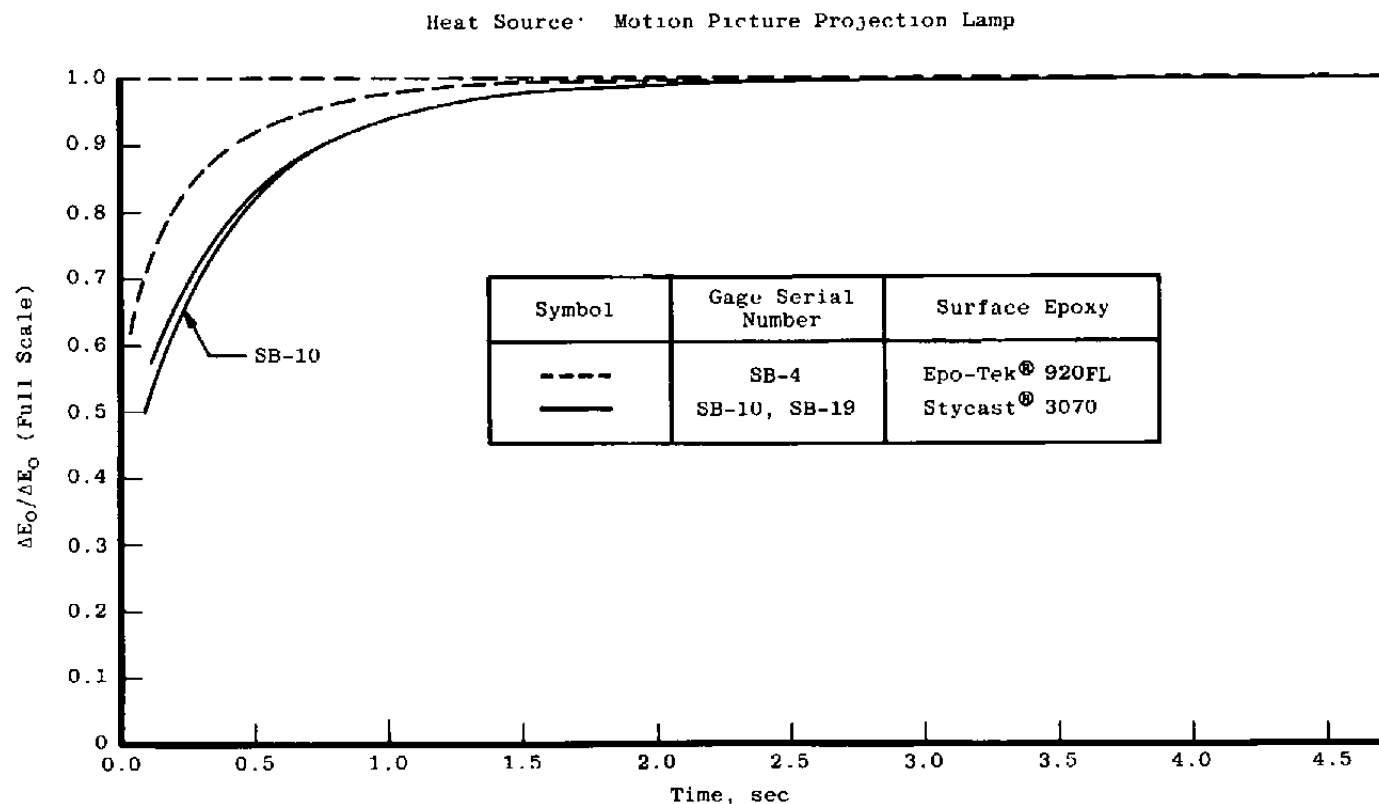
Figure 17. Normalized experimental time response of prototype Schmidt-Boelter gages.

Serial Number	Surface Epoxy
SB-4	Epo-Tek® 920FL
SB-19	Stycast® 3070

Measured Heat Flux

Measured Surface Temperature, SB-19

Measured Surface Temperature, SB-4

Measured Surface Temperature; 10 mil, 1/4-in.-diam Thermopile Gardon Gage

Measured Inside Gage Temperature

SB-19

SB-4

1/4-in.-diam Thermopile Gardon Gage

Time, sec

Figure 18. Measured temperature histories in heat transfer gages.
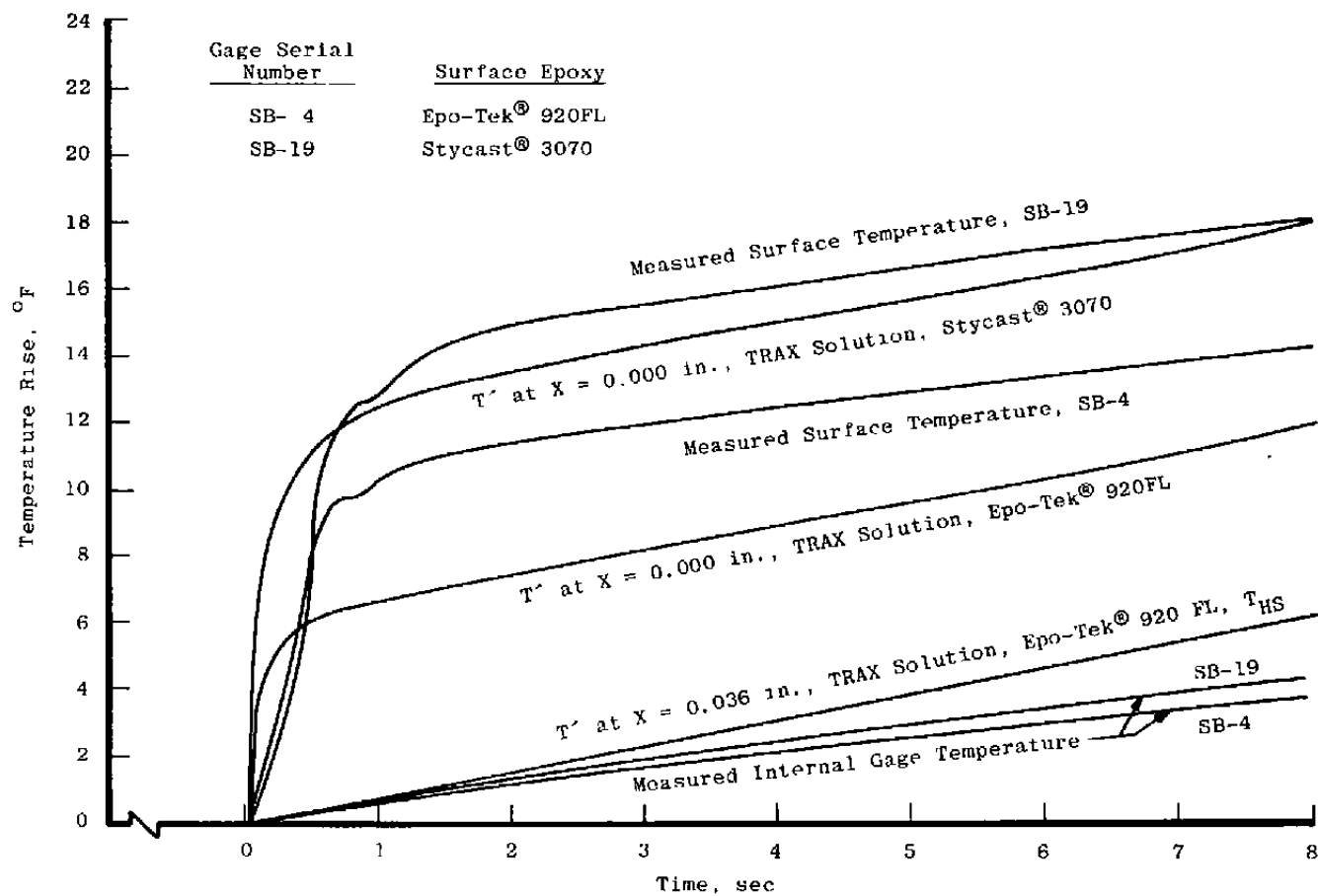
Figure 19. Comparison of measured and TRAX temperature distributions of Schmidt-Boelter gages.
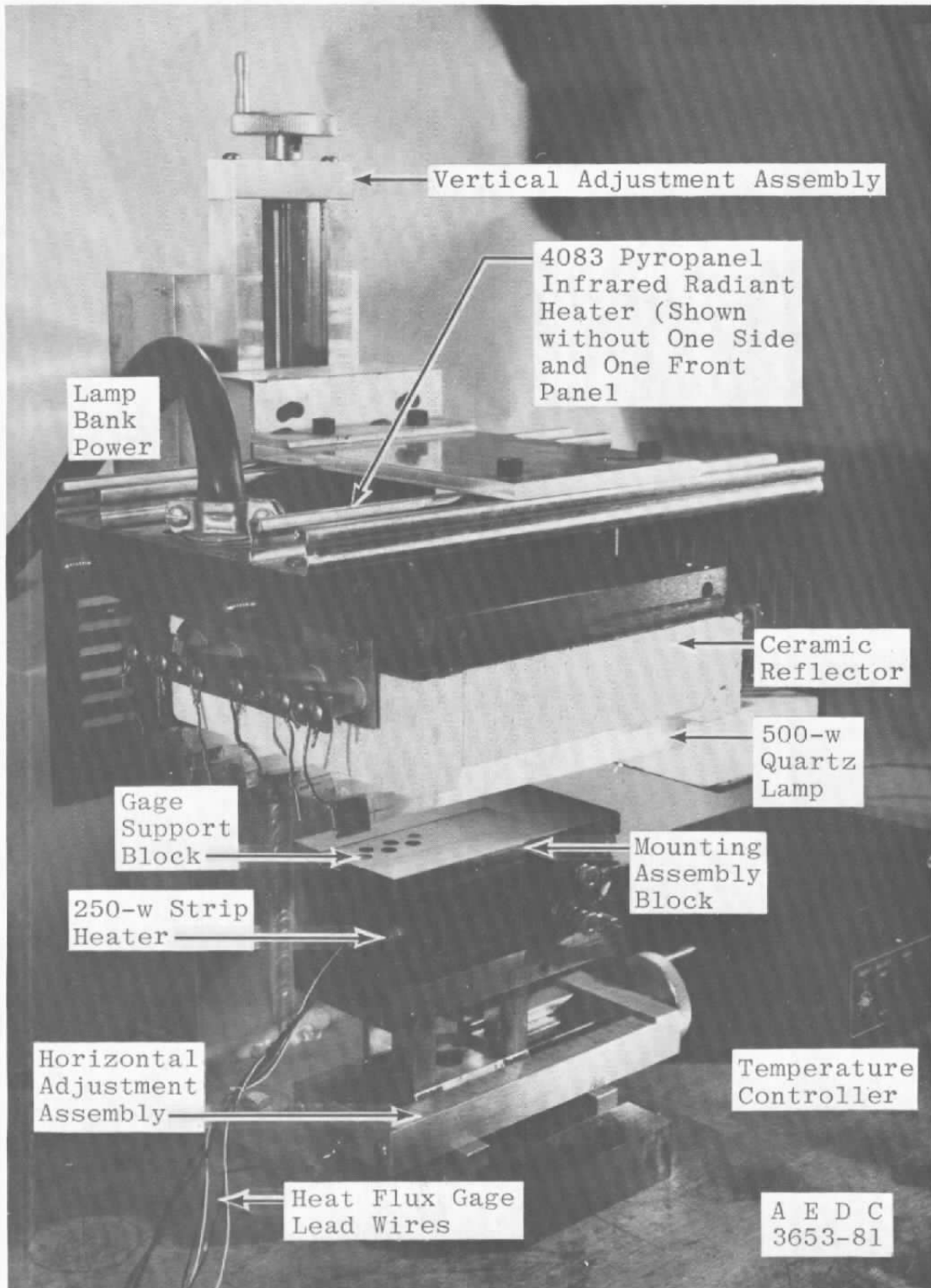
Figure 20. Heat flux gage radiant calibration system.
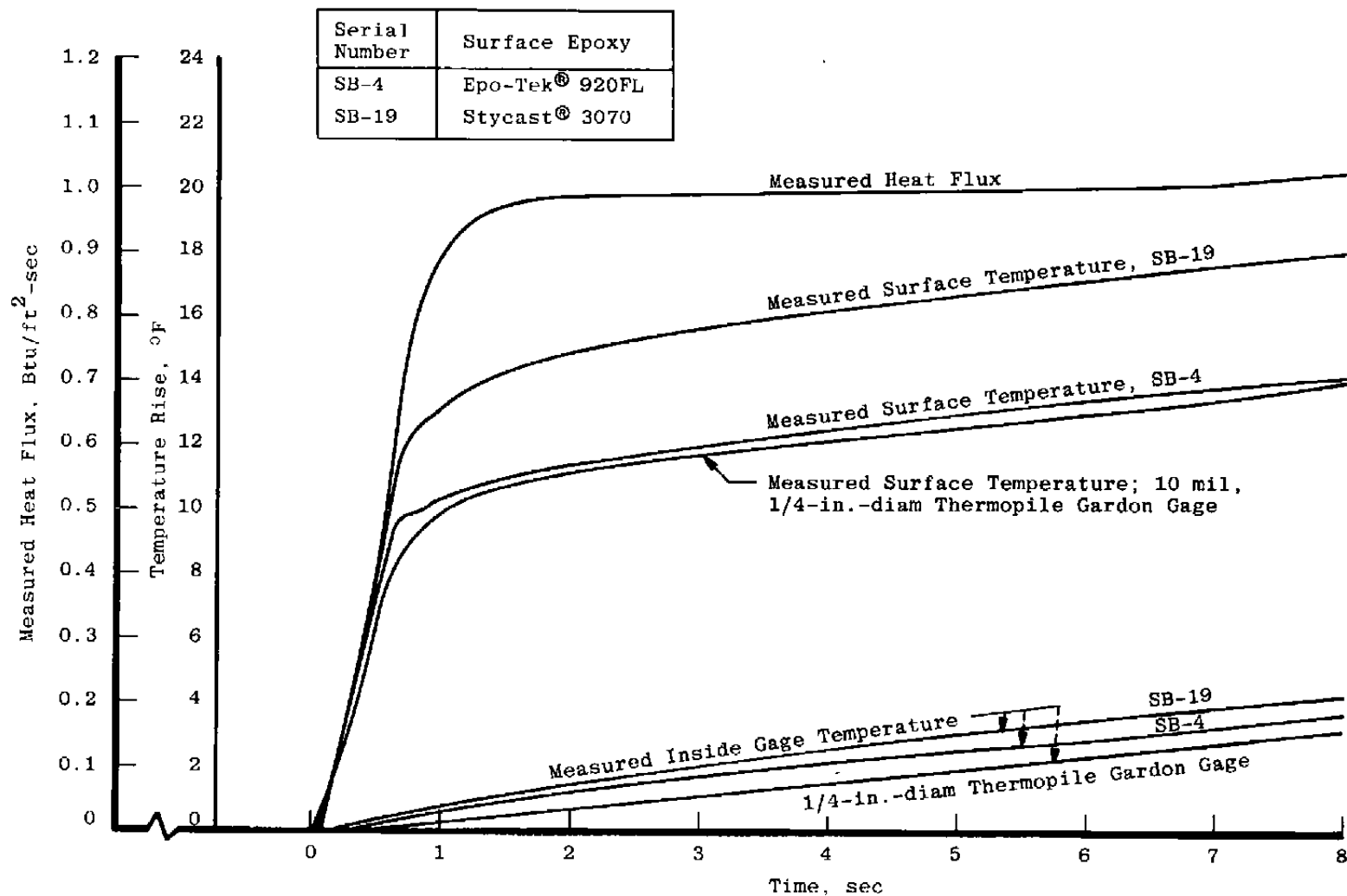
Vertical Adjustment Assembly

4083 Pyropanel Infrared Radiant Heater (Shown without One Side and One Front Panel)

Lamp Bank Power

Ceramic Reflector

500-w Quartz Lamp

Gage Support Block

Mounting Assembly Block

250-w Strip Heater

Horizontal Adjustment Assembly

Temperature Controller

Heat Flux Gage Lead Wires

A E D C
3653-81

Figure 21. Longitudinal heat flux map of quartz tube lamp bank.

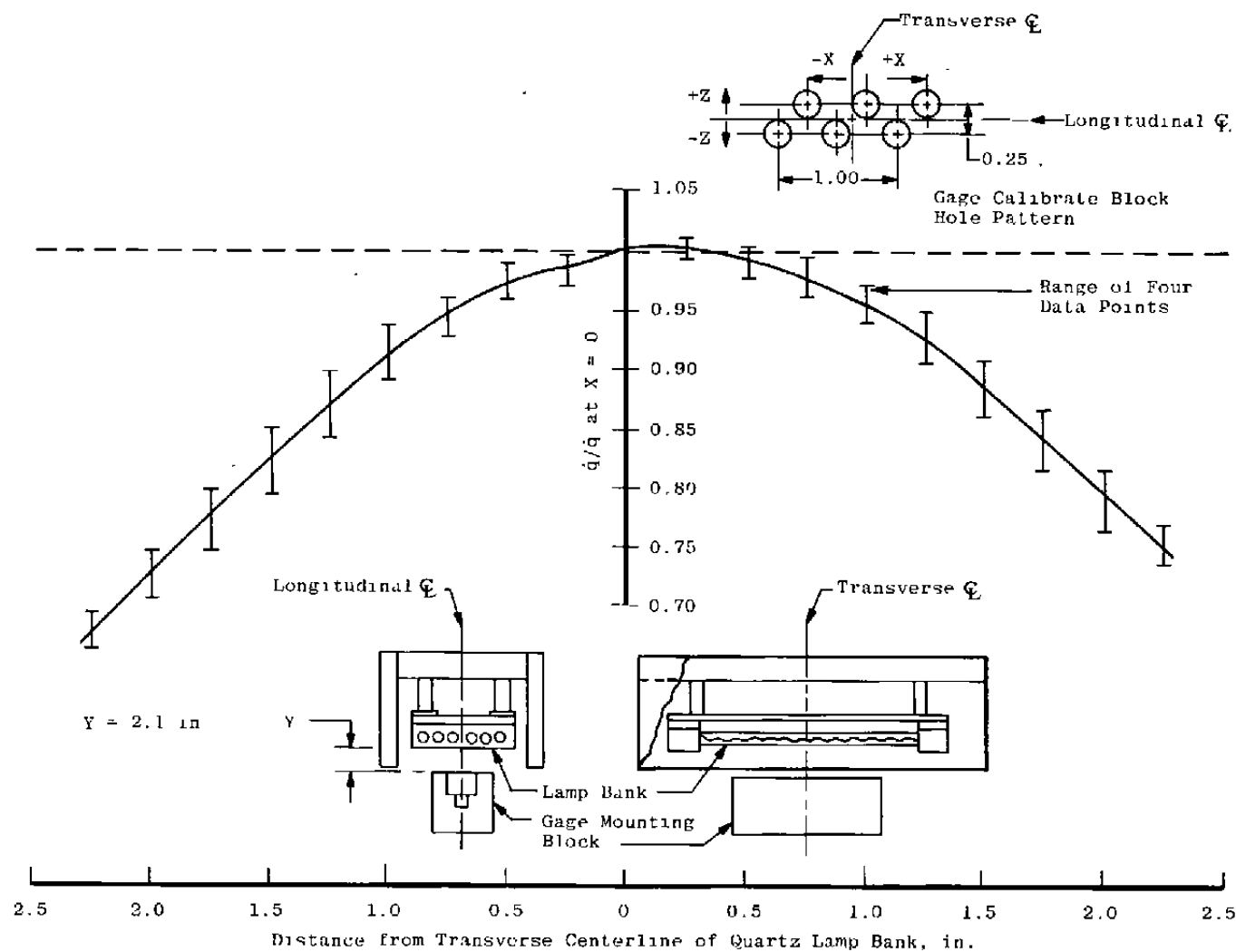The data acquisition system employed with this calibration facility consists of six d-c amplifiers, automatic timing circuitry, appropriate signal conditioning, a sample-and-hold operational amplifier, and a digital voltmeter. The system may be used in the manual timing mode or set to sample gage electrical output signals automatically at preset times from beginning of heating. Signals from transfer standard gages are routed through operational amplifiers with proper scaling resistors to indicate the calibration heat flux level in engineering units (Btu/ft^2-sec).

4.2.2 Procedures

Before beginning calibration procedures in a radiant heat flux calibration facility, a thin ($\cong$ 0.0005-in.) layer of high absorptivity coating is applied to the sensing surface of each heat flux sensor. The high absorptivity coating used at the AEDC/VKF is Krylon No. 1602 ultra-flat black spray enamel. The absorptivity of this coating has been experimentally checked several times with a Beckman® DK-2A spectroreflectometer and a Beckman Model IR-IV spectrophotometer and found to be 0.97 (± 1 percent deviation) over a wavelength range of 0.5 to 14 microns.

After applying the high absorptivity coating, up to four 1/4-in.-diam Schmidt-Boelter gages and two transfer standard gages are installed in a stainless steel gage support block. The gage support block is subsequently installed in a mounting assembly block. The lead wires are connected to the proper data acquisition system terminals. If the gages are to be calibrated at room temperature ambient conditions, a period of about 5 min is allowed for temperature stabilization. If the gages are to be calibrated at a higher ambient temperature condition, a longer stabilization time is required. After temperature stabilization has been attained, electrical power is applied to the lamp bank. If the system is operating in the automatic timing mode, all gage electrical output signals are simultaneously sampled at a preset time (usually 4 to 5 sec) from beginning of heating. Gage output signals (millivolts) and transfer standard indications (Btu/ft^2-sec) are recorded. This procedure is repeated for at least two heat flux levels for each transducer. The gage calibration scale factor, CSF (Btu/ft^2-sec/mv), is determined by dividing the indicated calibration heat flux level by the gage output.

4.2.3 Experimental Calibration Results

4.2.3.1 Room Temperature Ambient Conditions

Results of the experimental calibration of four prototype 1/4-in.-diam Schmidt-Boelter gages at room temperature ambient conditions are graphically illustrated in Fig. 22. These

calibrations were performed in accordance with procedures outlined in Sec. 4.2.2 and are typical of gage calibrations performed before a wind tunnel test. The full lines represent the best straight line curve fit through the four data points and zero for each gage. Since the abscissa is an indication of **absorbed** heat flux and the same high absorptivity coating was applied to the gages and transfer standards alike, the heat flux sensitivity of any particular gage is determined by measuring the slope of the straight line drawn through the individual data points. The calibration scale factor, CSF, is then merely the reciprocal of the heat flux sensitivity.

Figure 23 contains 14 experimental data points taken on two different days for one Schmidt-Boelter gage, SB-19. The full line between data points represents the best straight line curve fit. The mean value of the calibration scale factors represented by each data point and the standard deviation is shown in Fig. 23. This standard deviation represents repeatability or precision index for the data. Although not shown graphically, the mean value and standard deviation for up to 37 data points were calculated for the four gages listed in Fig. 22. These values are shown in Table 3. Individual data points used to determine calibration scale factor mean values and standard deviations shown in Table 3 were obtained over a time period of five days. These parameters were calculated using Eqs. (7) and (8), respectively (Ref. 16)

$$\overline{CSF} = \sum_{i=1}^{n} \frac{CSF_i}{n} \qquad (7)$$

$$S = \left(\sum_{i=1}^{n} \frac{CSF_i - \overline{CSF}}{n-1} \right)^{1/2} \qquad (8)$$

Table 3. Results of Schmidt-Boelter Gage Experimental Calibrations

Schmidt-Boelter Gage Serial Number	No. of Calibration Data Points	Mean Value of Calibration Scale Factor, CSF $(Btu/ft^2-sec/mv)$	Standard Deviation, (%)
SB-5	32	0.6589	0.840
SB-13	37	0.3078	1.25
SB-16	37	0.2917	0.963
SB-19	37	0.3363	0.773

NOTES:

1. All calibrations were performed at room temperature ambient conditions.

2. Calibration heat flux level varied from 0.6 to 8.2 Btu/ft^2-sec.

where CSF_i is an individual data point, $\overline{CSF}$ is the mean value of individual data points for one gage, n is the number of individual data points for one gage, and S is standard deviation or precison index for one gage.

Rather extensive experimental calibrations were recently (January 1981) conducted to determine the overall uncertainty in heat flux gage calibrations at the AEDC/VKF. Uncertainty is defined in Ref. 16:

$$U = \pm(B + t_{95}s) \tag{9}$$

where B is the system bias term and t is the 95th percentile point for the two-tailed Student's "t" distribution. The uncertainty of heat flux calibrations determined by the January 1981 experiments was 4.28 percent.

4.2.3.2 Elevated Ambient Temperature Calibrations

Experimental heat flux calibrations were performed simultaneously on four prototype Schmidt-Boelter gages at ambient temperatures up to 500°F in the following manner. Four 1/4-in.-diam gages and two transfer standard gages were installed in a gage support block which was subsequently installed in a mounting assembly block (Fig. 20). Calibrations were performed on these at one intermediate heat flux level (4 2 Btu/ft²-sec) at room temperature ambient conditions to establish a baseline calibration scale factor for each gage according to procedures given in Sec. 4.2.2. Taking care to maintain the same calibration heat flux level, the transfer standard gages were removed from the gage support block. Electrical power was supplied to the three heater strips attached to the mounting assembly block (Fig. 20) through a digital indicating temperature controller. The temperature of each gage was monitored with a digital scanning thermometer. When the desired ambient temperature level was attained and stabilized, the gages were irradiated with the preset heat flux level from the lamp bank. The calibration scale factor for each gage at the prevailing ambient temperature level was calculated by dividing the previously measured (and maintained) heat flux level by the gage electrical output signal. This experimental procedure was repeated for several ambient temperature levels up to 500°F for two separate gage heat-up periods on two different days.

The effects of an effective decrease in the radiant heat flux incident upon the sensing surface because of an increase in the transducer ambient temperature were considered. Calculations showed a variation in the incident heat flux level of less than 0.5 percent at temperatures up to 500°F.
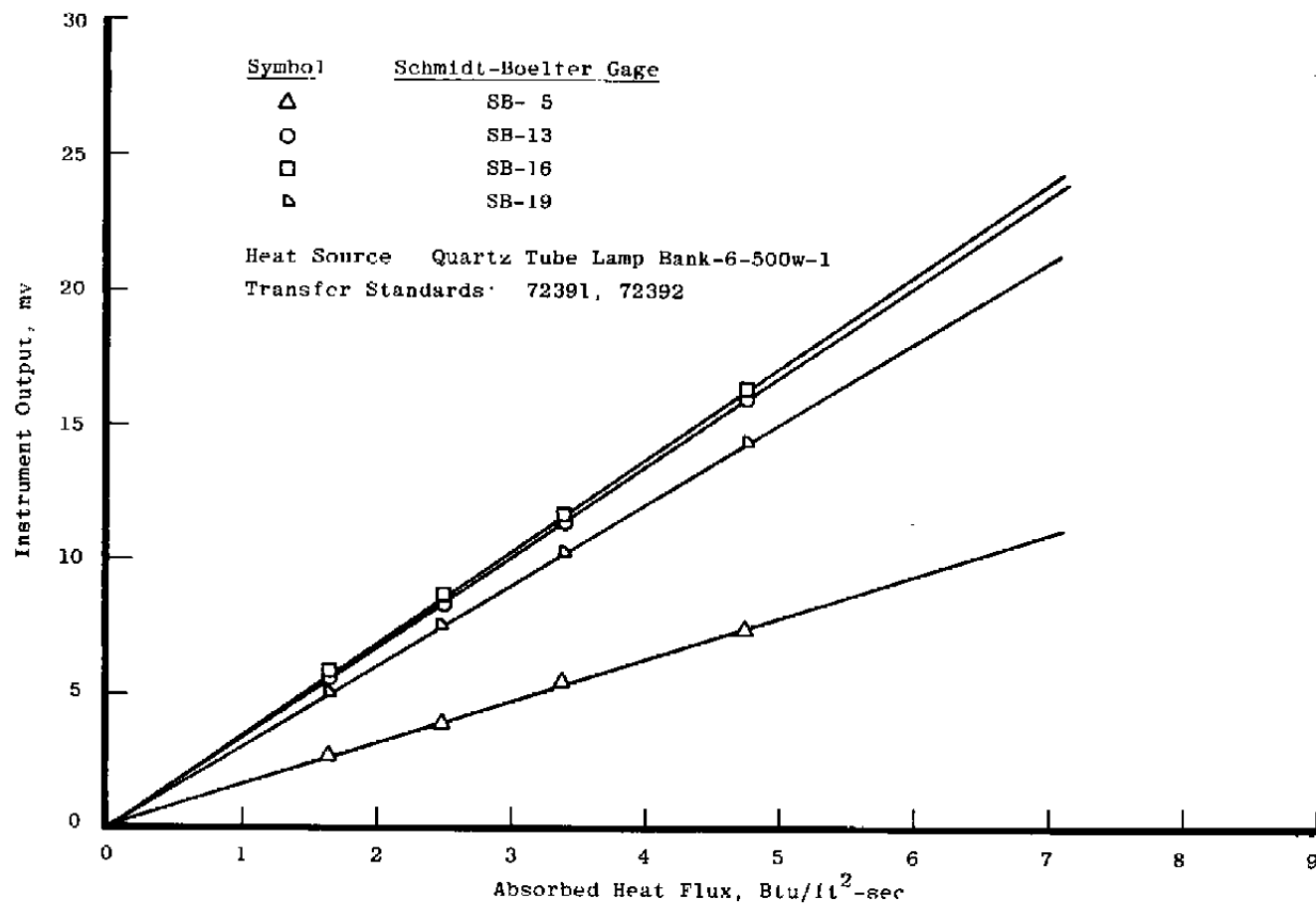
**Figure 22. Schmidt-Boelter gage calibration data at room temperature
ambient conditions.**

Heat Source   Quartz Tube Lamp Bank-6-500w-1
Transfer Standards   72391   72392

Schmidt-Boelter Gage-SB-19

⋈ May 7, 1981

△ May 11, 1981

Calibration Scale Factor, CSF, $\dfrac{Btu/ft^2\text{-sec}}{mv}$

Mean Value   0.3346

Standard Deviation   0.00224 (0.67%)

Instrument Output, mv (y-axis)

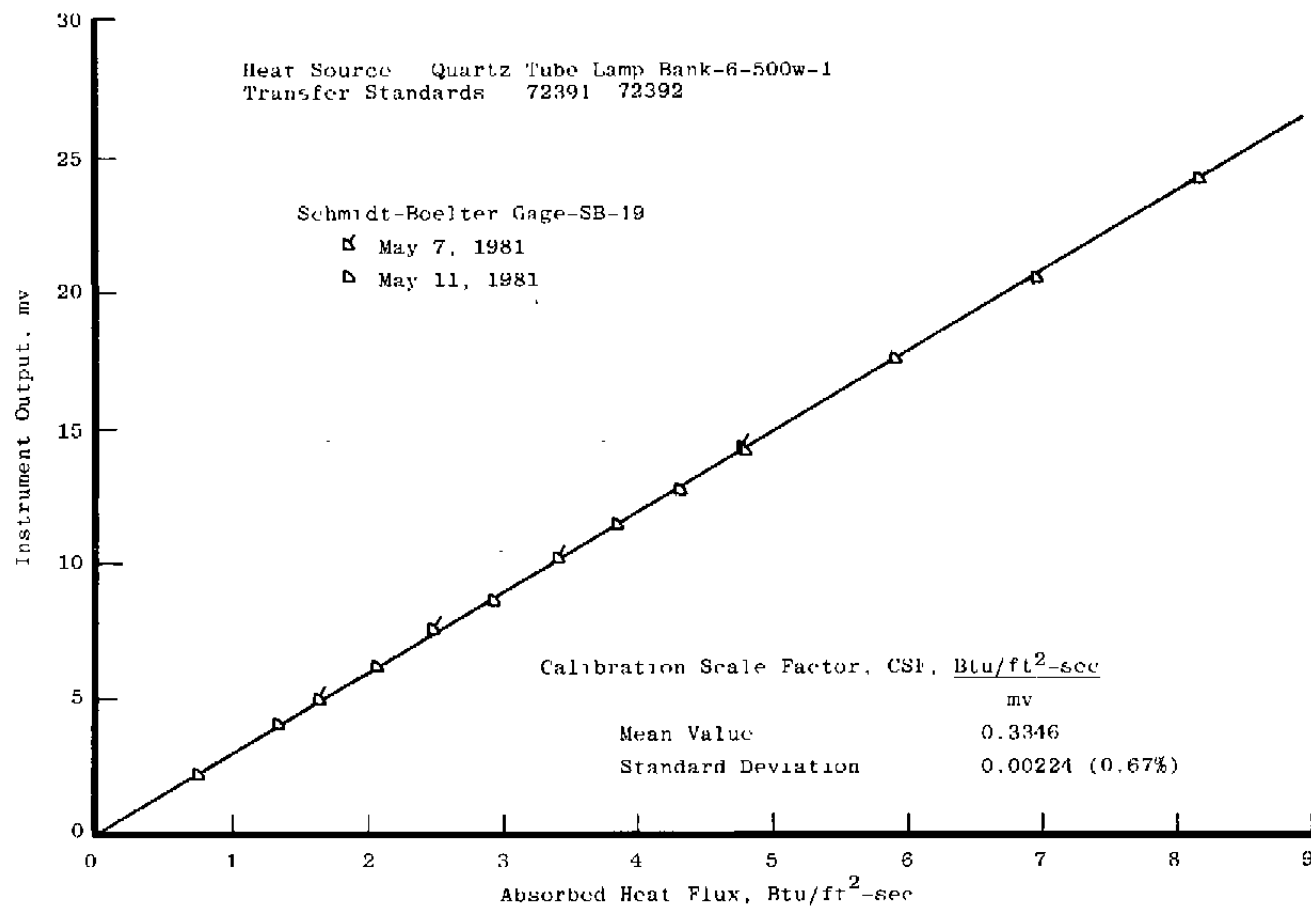Absorbed Heat Flux, Btu/ft^2-sec (x-axis)

Figure 23. Typical Schmidt-Boelter gage calibration data.

Results of the elevated ambient temperature calibrations are graphically shown in Fig. 24. It is obvious there is little change in Schmidt-Boelter gage calibration scale factor with ambient temperature up to temperatures of 500°F. In fact, there is no consistent change in calibration scale factor with temperature. There is slightly more scatter in the data at the higher temperatures because of increased sensitivity to room air currents, etc.

4.3 WIND TUNNEL TEST RESULTS

Heat flux gages fabricated according to the general Schmidt-Boelter concept have been evaluated in numerous AEDC/VKF continuous wind tunnel aerodynamic heating measurement applications. Since thermopile Gardon gages (Ref. 2) are generally used in discrete heat flux measurements, wind tunnel evaluations of prototype Schmidt-Boelter gages have usually been made by comparisons with Gardon gage data. Whenever possible, to obtain a valid comparison, efforts were made to locate one or more Schmidt-Boelter gages in the same relative locations (geometrically symmetrical) as Gardon gages on a test model. In several cases it was necessary to alternate Schmidt-Boelter gages with Gardon gages in an axial or transaxial distribution on the test model. The wind tunnel test data included in this report are heat flux and heat transfer coefficient distributions. Since all of the Schmidt-Boelter gage wind tunnel evaluations were made on a "piggyback" basis, all data will include relatively few Schmidt-Boelter gage data points compared with Gardon gage data points. All of the data shown were obtained on flat plate models where heat transfer distributions are well known.

Figures 25 and 26 show axial heat flux and heat transfer coefficient distributions on a flat plate model during a recent (April 1981) test in VKF Hypersonic Wind Tunnel (B) for three different tunnel runs. Thirteen 10-mil, 1/4-in.-diam thermopile Gardon gages and six 1/4-in.-diam Schmidt-Boelter gages were installed in the test model. The six Schmidt-Boelter gages represent the largest number of these gages evaluated in any single wind tunnel test to date at the AEDC/VKF. Axial centerline heat flux distributions (circular symbols) from two different tunnel runs are graphically illustrated in Fig. 25. Off centerline data (square and triangular symbols) are also shown in Fig. 25. The wedge angle was 8.36 deg for Run No. 1 and 14.94 deg for Run No. 2. Other tunnel conditions were the same and are indicated in Fig. 25. Gardon gage data are represented by the open symbols and the Schmidt-Boelter gage data by the closed symbols. Data were sampled at time points of 58.8 and 9.95 sec from model injection into the tunnel flow for Runs No. 1 and No. 2, respectively. There is good agreement between Gardon and Schmidt-Boelter gage data over a range from about 0.8 to 1.8 Btu/ft^2-sec.
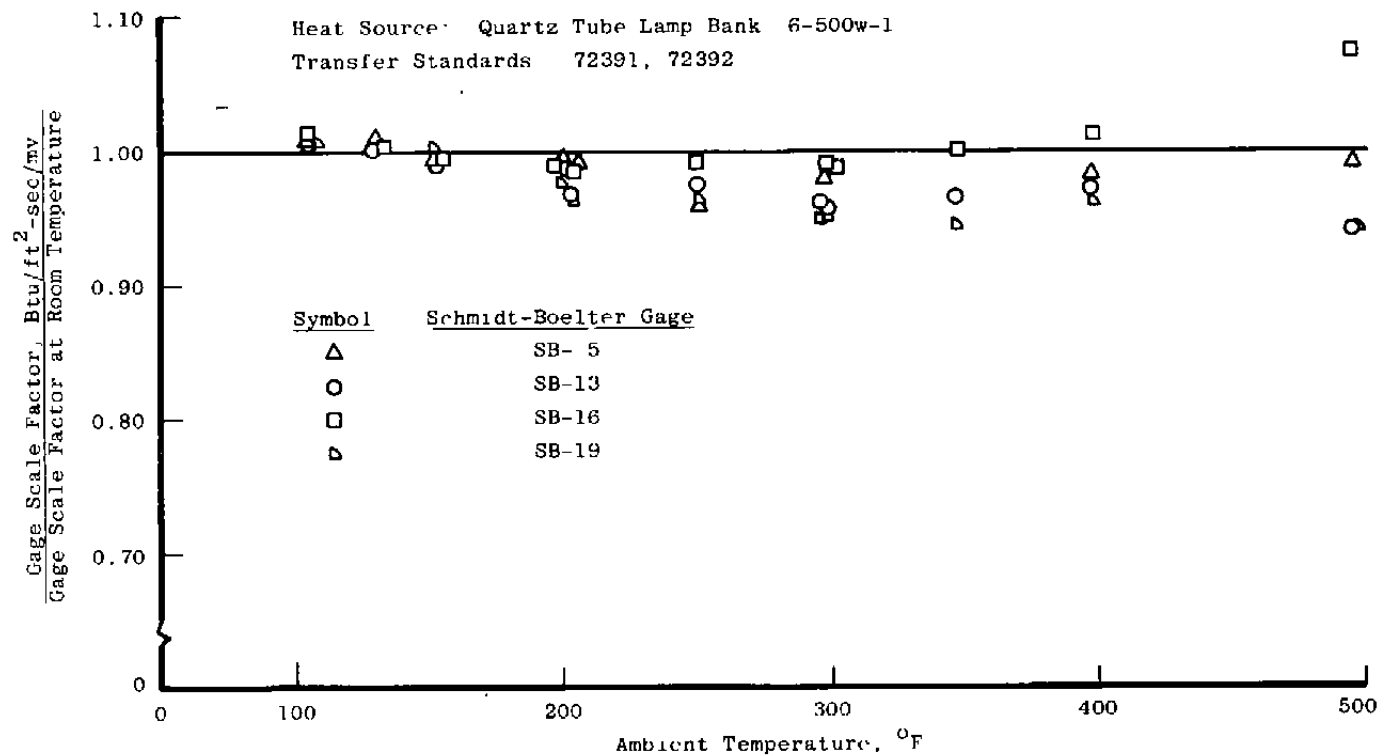
Figure 24. Variation of Schmidt-Boelter gage calibration scale factor with ambient temperature.
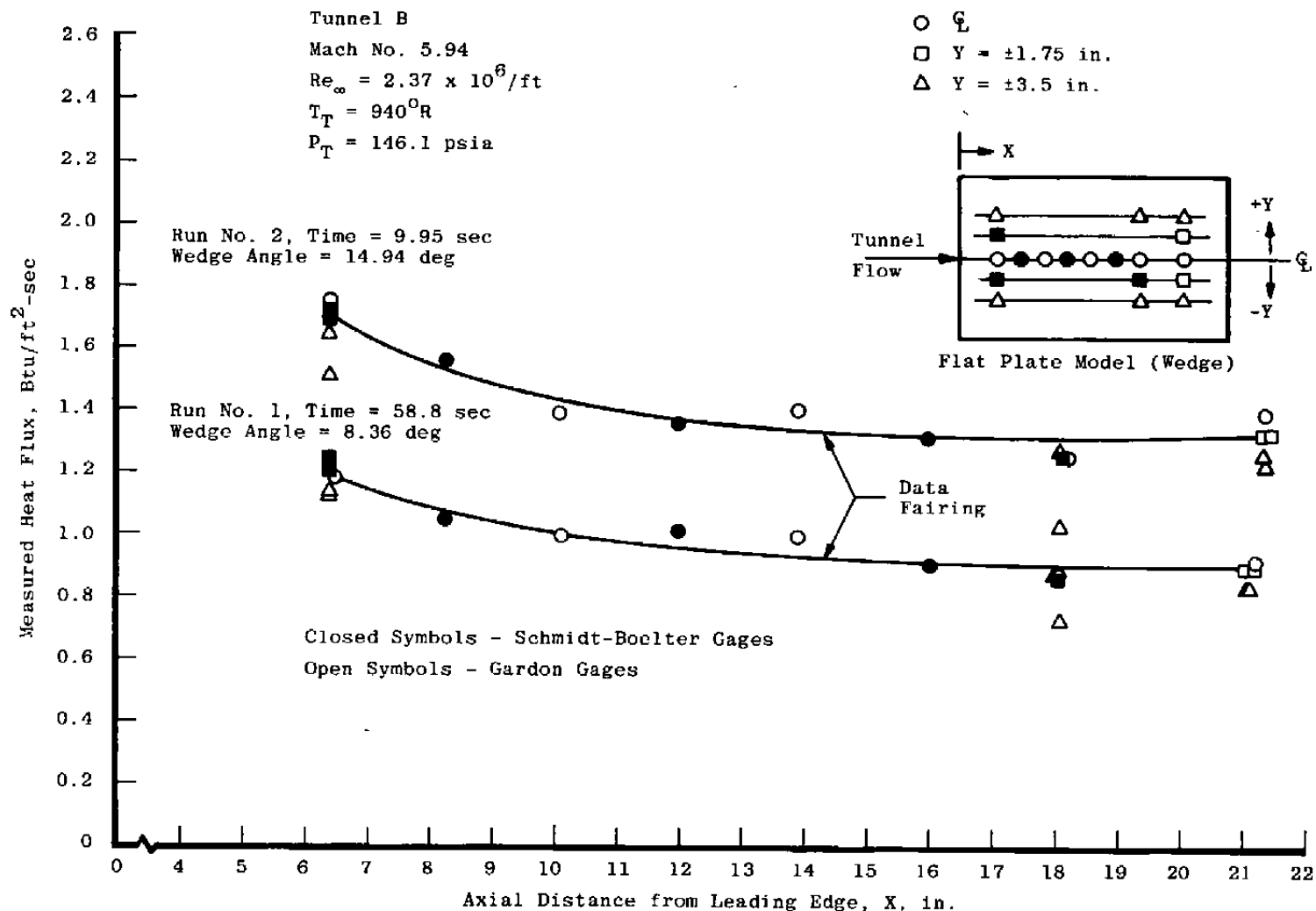
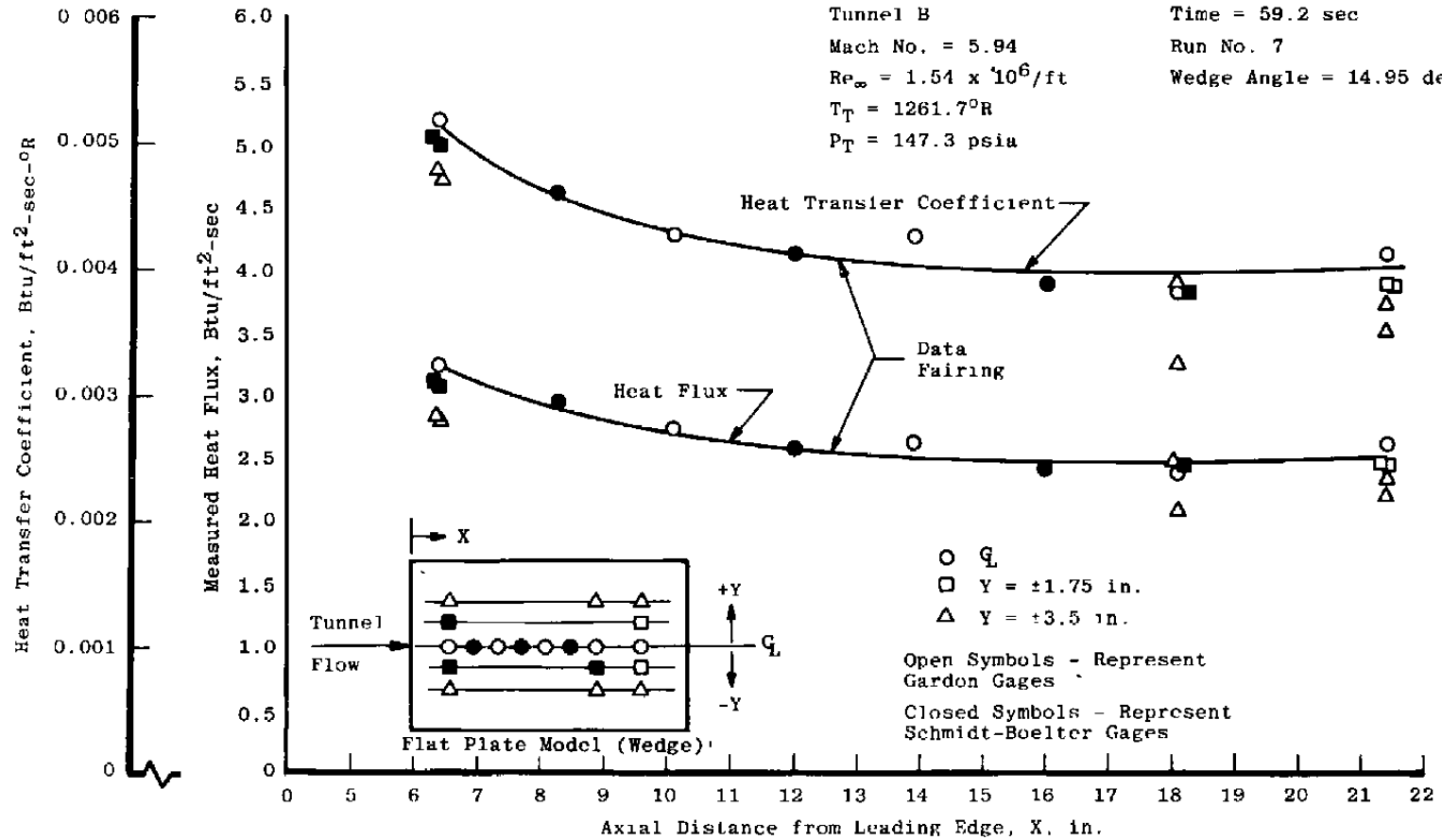**Figure 25. Axial heat flux distribution on a flat plate model.**

Figure 26. Axial heat transfer distribution on a flat plate model.

Figure 26 is an axial heat transfer distribution for another tunnel run. Pertinent tunnel condition information is listed on the illustration. Two different plots are shown in Fig. 26. These are heat flux and heat transfer coefficient distributions. As expected, the two plots show good symmetry and there is good agreement between Gardon and Schmidt-Boelter gage data. The relationship between heat flux and heat transfer coefficient is given by Eq. (3).

A wind tunnel test with a model instrumented with three 1/4-in.-diam Schmidt-Boelter gages and 79 thermopile Gardon gages was run in VKF Tunnel B in April 1981. A Gardon gage was located at a model position geometrically symmetrical (mirror image) with each Schmidt-Boelter gage installation. Sixty Tunnel B runs were made at model angles of attack varying from 0 to 20 deg. Heat flux levels varying from 0.06 to 6.0 Btu/ft²-sec were measured with the Schmidt-Boelter gages. Good agreement with Gardon gage data at geometrically symmetrical model locations was obtained with all three Schmidt-Boelter gages at all run conditions. Data and a model sketch from this test were not shown in this report because of security classification restrictions.

The wind tunnel test described in the preceding paragraph involved a relatively large number of heat flux gages (82) and tunnel runs (60). At the end of the test, seven thermopile Gardon gages were either nonoperational or were giving questionable results. This is not a large number of failures, and test objectives were not compromised. However, it should be noted that during wind tunnel evaluations of prototype Schmidt-Boelter gages, covering about three years, there has never been an operational gage failure. Under normal wind tunnel test conditions below 600°F, it is expected that the Schmidt-Boelter gage should be nearly indestructible.

5.0 CONCLUSIONS

Significant progress has been made in the development of a heat flux transducer whose principle of operation is based on the Schmidt-Boelter or axial temperature gradient concept, for continuous flow wind tunnel measurement applications. The transducer features excellent durability, a self-generating and direct-reading electrical output signal, a maximum continuous service temperature of 600°F, and limited contourability. A finite-element, two-dimensional heat conduction computer code, TRAX, which provides analytical data which are in good agreement with experimental results, has been effectively employed in the design and development of the transducer. Several prototype gages have been fabricated and subsequently evaluated in laboratory and continuous wind tunnel test applications. Laboratory tests have shown the gages to have excellent calibration stability and calibration scale factors are essentially independent of temperature through the entire

service temperature range. Numerous wind tunnel test evaluations have been conducted without a single gage casualty or gage related operational problem. Good agreement with Gardon gage wind tunnel test data has been achieved at heat flux levels from ≤ 0.1 to 10 Btu/ft^2-sec.

It is anticipated that the successful development of the Schmidt-Boelter gage for continuous wind tunnel aerodynamic heat transfer measurements will result in the gradual replacement of conventional and thermopile Gardon gages in most applications at the AEDC/VKF. There are also test conditions for which Schmidt-Boelter gages would appear to be a viable alternative for coaxial surface thermocouples and thin skin thermocouples. The excellent durability and versatility of the gage make it a prime candidate for flight vehicle measurements and radiation heat transfer applications.

The gage described in this report is not an optimum design for all measurement requirements in the AEDC/VKF. However, the results of the work described should enable the experimental aerodynamicist to design a gage which will provide accurate data in most continuous flow wind tunnel heat transfer measurement applications. Regarding the future development of the Schmidt-Boelter gage, there are several areas in which additional work is needed. These include the following:

1. Extensive surface temperature measurements of prototype gages under controlled laboratory conditions,

2. Thorough analysis of the effect of surface temperature perturbations or discontinuities on the model or test article surface,

3. Investigation of the feasibility of decreasing gage size (outside diameter) to 0.187 or 0.125 in., and

4. Investigation of alternate methods of sensing temperature differences in the wafer.

REFERENCES

1. *Test Facilities Handbook.* (Eleventh Edition). "von Kármán Gas Dynamics Facility, Vol. 3," Arnold Engineering Development Center, June 1979.

2. Trimmer, L. L., Matthews, R. K., and Buchanan, T. D. "Measurement of Aerodynamic Heat Rates at the AEDC von Kármán Facility." 5th International Congress on Instrumentation in Aerospace Simulation Facilities, September 1973.

3. Ledford, R. L., Smotherman, W. E., and Kidd, C. T. "Recent Developments in Heat-Transfer-Rate, Pressure, and Force Measurements for Hotshot Tunnels." AEDC-TR-66-228 (AD645764), January 1967.

4. Stallings, D. W., Matthews, R. K., and Jenke, L. M. "Recent Developments in Aerothermodynamic Test Techniques at the AEDC von Kármán Gas Dynamics Facility." 8th International Congress on Instrumentation in Aerospace Simulation Facilities, September 1979.

5. Baines, D. J. "A Comparative Theoretical Evaluation of Five Commonly Used Types of Unsteady Heat Flux Sensor." Department of Supply, Australian Defense Scientific Service, Weapons Research Establishment Report HSA27, January 1970.

6. Carnahan, K. R., Hartman, G. J., and Neuner, G. J. "Development of TPS Flight Test and Operational Instrumentation," Aerotherm Report FR-75-135, January 1975.

7. Hager, N. E. "Thin Foil Heat Meter," *The Review of Scientific Instruments*, Vol. 36, No. 11, November 1965.

8. Rochelle, J. K. "TRAX -A Finite Element Computer Program for Transient Heat Conduction Analysis of Axisymmetric Bodies." University of Tennessee Space Institute Master's Thesis, June 1973.

9. Liepmann, H. W. and Roshko, A. *Elements of Gasdynamics,* John Wiley and Sons, Inc., New York, 1957.

10. Woodruff, L. W., Hearne, L. F., and Keliher, T. J. "Interpretation of Asymptotic Calorimeter Measurements." AIAA Journal, Vol. 5, No. 4, April 1967, pp. 795-797.

11. Schultz, D. L. and Jones, T. V. "Heat-Transfer Measurements in Short-Duration Hypersonic Facilities." AGARD-AG-165, February 1973.

12. Hornbaker, D. R. and Rall, D. L. "Design and Performance Considerations for Thermal Radiation Measuring Instruments." ISA Reprint TR-194, October 1965.

13. Carslaw, H. S. and Jaeger, J. C. *Conduction of Heat In Solids.* Clarendon Press, Oxford, 1959, (Second Edition).

14. Ozisik, M. N., *Boundary Value Problems of Heat Conduction.* International Textbook Company, Scranton, PA, 1968.

15. Brown, H. K. "The Theoretical Response of Heat Transfer Gages Employed in Shock Tubes." AVCO Research Note 58, February 1958.

16. Abernethy, R. B. et al. and Thompson, J. W. "Handbook Uncertainty in Gas Turbine Measurements." AEDC-TR-73-5 (AD755356), February 1973.

APPENDIX A
DERIVATION OF STEADY-STATE HEAT FLUX SENSITIVITY
OF THE SCHMIDT-BOELTER GAGE

Consider the mathematical model of a parallel wall slab backed by a semi-infinite solid (see Fig. 6). The surface temperature, $T_{o,t}$ is given by the following expression (Ref. 12):

$$T_{o,t} = \frac{2\dot{q}_o (k_1 t)^{1/2}}{\pi^{1/2} K_1} + \frac{4\dot{q}_o (k_1 t)^{1/2}}{K_1} \sum_{n=1}^{\infty} b^n \text{ierfc} \frac{2n\ell}{2(k_1 t)^{1/2}} \qquad (A-1)$$

Expanding Eq. (A-1) yields

$$T_{o,t} = \frac{2\dot{q}_o (k_1 t)^{1/2}}{\pi^{1/2} K_1} + \frac{4\dot{q}_o (k_1 t)^{1/2}}{K_1} \qquad (A-2)$$

$$\sum_{n=1}^{\infty} b^n \left(\frac{1.0}{\pi^{1/2} e^{n^2 \ell^2 / k_1 t}} - \frac{n\ell}{(k_1 t)^{1/2}} \text{erfc} \frac{n\ell}{(k_1 t)^{1/2}} \right)$$

The temperature at the interface, $X_1 = \ell$, is represented by

$$T_{\ell,t} = 2\dot{q}_o (k_1 t)^{1/2} \text{ierfc} \frac{\ell}{2(k_1 t)^{1/2}} + \qquad (A-3)$$

$$\frac{2\dot{q}_o (k_1 t)^{1/2}}{K_1} \sum_{n=1}^{\infty} b^n \left[\text{ierfc} \frac{(2n-1)\ell}{2(k_1 t)^{1/2}} + \text{ierfc} \frac{(2n+1)\ell}{2(k_1 t)^{1/2}} \right]$$

Expanding Eq. (A-3) yields

$$T_{\ell,t} = \frac{2\dot{q}_o (k_1 t)^{1/2}}{K_1} \left[\frac{1.0}{\pi^{1/2} e^{\ell^2 / 4k_1 t}} - \frac{\ell}{2(k_1 t)^{1/2}} \cdot \text{erfc} \frac{\ell}{2(k_1 t)^{1/2}} \right] + \qquad (A-4)$$

$$\frac{2\dot{q}_o (k_1 t)^{1/2}}{K_1} \sum_{n=1}^{\infty} b^n \left[\frac{1.0}{\pi^{1/2} e^{(2n-1)^2 \ell^2 / 4k_1 t}} - \frac{(2n-1)\ell}{2(k_1 t)^{1/2}} \text{erfc} \frac{(2n-1)\ell}{2(k_1 t)^{1/2}} + \right.$$

$$\left. \frac{1.0}{\pi^{1/2} e^{(2n+1)^2 / 4k_1 t}} - \frac{(2n-1)\ell}{2(k_1 t)^{1/2}} \cdot \text{erfc} \frac{(2n+1)\ell}{2(k_1 t)^{1/2}} \right]$$

59

Consider the case for which the slab and backing materials are the same:

$$a = 1.0, \ b = 0.0$$

$$T_{o,t} = \frac{2\dot{q}_o (k_1 t)^{1/2}}{\pi^{1/2} K_1} \tag{A-5}$$

$$T_{\ell,t} = \frac{2\dot{q}_o (k_1 t)^{1/2}}{K_1} \left(\frac{1.0}{\pi^{1/2} e^{\ell^2/4k_1 t}} - \frac{\ell}{2(k_1 t)^{1/2}} \ \text{erfc} \ \frac{\ell}{2(k_1 t)^{1/2}} \right) \tag{A-6}$$

Combine Eq. (A-5) with Eq. (A-6) to obtain the temperature difference between front surface and interface:

$$T_{o,t} - T_{\ell,t} = \frac{2\dot{q}_o (k_1 t)^{1/2}}{\pi^{1/2} K_1} - \frac{2\dot{q}_o (k_1 t)^{1/2}}{K_1} \left(\frac{1.0}{\pi^{1/2} e^{\ell^2/4k_1 t}} - \frac{\ell}{2(k_1 t)^{1/2}} \ - \right.$$

$$\left. \frac{\ell}{2(k_1 t)^{1/2}} \ \text{erfc} \ \frac{\ell}{2(k_1 t)^{1/2}} \right) \tag{A-7}$$

Rearranging Eq. (A-7) yields

$$T_{o,t} - T_{\ell,t} = \frac{2\dot{q}_o (k_1 t)^{1/2}}{\pi^{1/2} K_1} \left(1.0 - \frac{1.0}{e^{\ell^2/4k_1 t}} \right) + \frac{\dot{q}_o \ell}{K_1} \ \text{erfc} \ \frac{\ell}{2(k_1 t)^{1/2}} \tag{A-8}$$

Let time, t, approach infinity:

$$T_{o,t} - T_{\ell,t} = \frac{2\dot{q}_o (k_1 t)^{1/2}}{\pi^{1/2} K_1} \left(1.0 - \frac{1.0}{e^{\ell^2/4k_1 t}} \right) \ + \ \frac{\dot{q}_o \ell}{K_1} \ \text{erfc} \ \frac{\ell}{2(k_1 t)^{1/2}} \tag{A-9}$$

$$T_{o,t} - T_{\ell,t} \ \text{(steady state)} = \frac{\dot{q}_o \ell}{K_1} \tag{A-10}$$

NOMENCLATURE

a	$K_2/K_1 (k_1/k_2)^{1/2}$
B	Bias term
b	$(1-a)/(1+a)$
C_p	Specific heat, Btu/lb-°F
CSF	Calibration scale factor of heat flux gage, Btu/ft²-sec/mv
E	Electromotive force, v
erfc	Complementary error function
h	Heat transfer coefficient, Btu/ft²-sec-°F
ierfc	Complementary integral error function
K	Thermal conductivity, Btu/ft-sec°F
k	Thermal diffusivity, $(K/\varrho C_p)$, ft²/sec
ℓ	Thickness of slab or wafer, ft
M	Mach number
N	Number of turns on wafer of Schmidt-Boelter gage
n	Number in infinite series
P_T	Tunnel stilling chamber pressure, psia
$\dot{q}$	Heat flux or heat-transfer-rate, Btu/ft²-sec
$\dot{q}_o$	Constant heat flux at surface, Btu/ft²-sec
R	Radial distance from axial centerline, ft
r	Recovery factor
RE	Reynolds number/ft
S	Precision index
T	Temperature, °F or °R
t	Time, sec

t_{95} Ninety-fifth percentile point for two-tailed Students' "t" distribution

T_T Tunnel stilling chamber temperature, °R

T' Temperature rise, °F or °R

U   Uncertainty

X   Axial distance, ft

X' Changed distance in axial direction, ft

α Angle of attack of wind tunnel test article, deg

δ Thermoelectric output sensitivity of thermocouple, mv/°F

ϱ Density, lb/ft³

ΔE_o Gage output signal, mv

ΔT Temperature difference, °F or °R

SUBSCRIPTS

1   Material number 1

2   Material number 2

o   Initial condition

C   Cold surface

H   Hot surface

ℓ Thickness of slab or wafer

r   Recovery

T   Total temperature

t   Time

X   Axial direction

w   Wall

∞ Free-stream condition